Accepted Manuscript

Title: Self-exciting vibrations and Hopf's bifurcation in non-linear stability analysis of rail vehicles in a curved track

Authors: Krzysztof Zboinski, Miroslaw Dusza

PII: S0997-7538(09)00118-1

DOI: 10.1016/j.euromechsol.2009.10.001

Reference: EJMSOL 2553

To appear in: *European Journal of Mechanics / A Solids*

Received Date: 23 November 2007

Revised Date: 30 September 2009

Accepted Date: 1 October 2009

Please cite this article as: Zboinski, K., Dusza, M. Self-exciting vibrations and Hopf's bifurcation in non-linear stability analysis of rail vehicles in a curved track, European Journal of Mechanics / A Solids (2009), doi: 10.1016/j.euromechsol.2009.10.001

Self-exciting vibrations and Hopf's bifurcation in non-linear stability analysis of rail vehicles in a curved track

Running title: Stability analysis of rail vehicles in a curved track

Authors: **Krzysztof Zboinski** and **Miroslaw Dusza**

Affiliation and address for both: Warsaw University of Technology,
Faculty of Transport,
Koszykowa 75,
00-662 Warsaw,
Poland

(Krzysztof Zboinski – corresponding author): tel. +48 22 234-70-78
fax +48 22 425-65-43
e-mail: kzb@it.pw.edu.pl

Abstract – the main objective of this article is to present the authors' view of- and results on non-linear lateral stability of rail vehicles in a curved track. Three elements are exploited in order to secure this objective. Firstly, physical genesis of the problem is discussed, and its similarity to straight track analysis is emphasized. Results of the theories of self-exciting vibrations and bifurcation are the key elements here. Secondly, the method suitable for analysis in a curved track is presented. New necessary elements, extending the better established methods for straight track are clearly mentioned and described. The methodology of building original stability maps, being the basis for the analysis and valid for whole range of curve radii and straight track is represented. Thirdly, a sample of the analysis is shown in order to give the idea how the method can be utilised. The case study refers to the influence of wheel/rail profiles on the stability in circularly curved track and straight track as well. Two different pairs of wheel/rail profiles are used and the corresponding results compared. The main contributions of the article are: a discussion of the physical nature of phenomena related to the stability in a curved tracks, and the method (procedure) established for the reasons of the analysis. Another and more general contribution is our say in the hot polemics on the advisability of stability analysis in curves and the advantages of the non-linear critical speed over the linear one.

Keywords: railway vehicle dynamics, non-linear stability, curved track, numerical simulation

1. Introduction

This article results from and continues many years' interest of the authors in dynamics of rail vehicles in a curved track. In particular, this interest is focused on studies of the limit cycles and the stability of motion of rail vehicles, which is the basic substance of the paper. The considerations and results presented are to some extent the continuation of those started earlier by Zboinski (1998). An important contribution of that publication was putting the problem of rail vehicles stability in a curved track, explicitly. Many detailed questions were put there, too. Quite a few of them remained open at that time. Now, after nine years passed, some of the questions have been answered thanks to the works of many researchers, including authors of this paper. However, there are still open issues that are continually a matter of intensive studies or require persistent suppressing the stereotypes, despite the fact that many qualitatively new results were published.

A question of that sort is the analysis of rail vehicles stability in a curved track. In spite of putting the problem explicitly (Zboinski, 1998) and later explicit studies, both by the authors of this article (Zboinski and Dusza, 2002, 2004-a, 2004-b, 2006; Dusza, 2005) and others (True and Birkedal Nielsen, 1998; Lee and Cheng, 2003, 2005, 2006-a, 2006-b; True at al., 2005; Lee at al., 2005; Hoffmann, 2006; Hoffmann and True, 2008; and Zeng and Wu, 2004, 2005), a group of researchers and railway practitioners exists considering the hunting motion either to be absent in a curved track or to be unworthy of interest (consequently the stability). They advocate traditional opinion that periodic vibrations of constant amplitude (limit cycles) above critical velocity appear for straight track only, whereas in circular curves the motion is purely of quasi-static character.

Similar situation takes place in case of stability analysis in a straight track. There is a traditional opinion that in order to determine the value of critical velocity it is enough to employ linear model of vehicle. In particular linear geometry of wheel/rail contact is applied,

where so-called equivalent conicity (Elkins, 1992) has got key significance. Critical velocity obtained in such conditions is often called linear one and denoted v_c. On the other hand a great number of the works indicates existence of Hopf bifurcation and attractor, determining so-called non-linear critical velocity v_n (Xu at al., 1992; Jensen and True, 1997; True and Jensen, 1994-b; Zboinski, 1998; Knothe and Böhm, 1999; Lee and Cheng, 2003, 2005; Shupp, 2004; Zeng and Wu, 2004, 2005; Zboinski and Dusza, 2004-a, 2006; Dusza, 2005; Hoffmann, 2006; and Polach, 2006). Its value is different in general from linear velocity v_c and physical nature of v_n and v_c is different, too. Despite these the traditional approach ignoring influence of non-linearity holds itself well, and new views reveal themselves with difficulty in some societies. It is like that, although this problem is publicly and explicitly discussed (for instance by True, 1994; Knothe and Böhm, 1999; and Goodall and Iwnicki, 2004). It seems that such state of affairs arises from insufficient understanding of self-exciting vibrations theory, bifurcation theory and questions of chaos, especially by railway practitioners. Therefore, the easier and more engineering methods (e.g. Wickens, 1965-a, 1965-b; Shen, 1992; and Dukkipati, 1994) based on linear models and linear methods of stability studies (eigen values analysis) still find many followers. The works of True and his co-authors (e.g. True and Birkedal Nielsen, 1998; True, 1992, 1999, 2006; True and Jensen, 1994-a, 1994-b; True at al., 1996, 2005; Jensen and True, 1997; Hoffmann and True, 2008) occupy remarkable place in the propagation and development of non-linear mechanics (and in particular of stability) methods in the railway vehicle dynamics. Most of these works deal with straight track analysis, some however refer to curved track case.

In our opinion, most works concerning stability in curves (also those already mentioned in this article) has got one disadvantageous feature in terms of braking down the traditional view on stability. They focus, namely on selected dynamical feature(s) of particular railway vehicle. However, they insufficiently explain the origin and physics of the

phenomena, and just indirectly refer to non-linear methods of stability studies in straight track, which are wider spread in the society. From that point of view, the reference by (Zboinski, 1998) is still important because it relates to these problems in direct way. The described state of affairs is in our view one of the reasons for slow spreading the opinion about usefulness of the stability studies in a curved track. Improving that state is the main motivation for elaboration of this paper and the main objective, at the same time.

In consideration of the identical physical nature of self-exciting vibrations in a curve, as in a straight track (ST), including the same sense of non-linear critical velocity v_n (Zboinski and Dusza, 2004-a, 2004-b, 2006; Dusza, 2005), the current article realises also a supplementary objective. It is our support to those who point at higher accuracy, and this way at the superiority of determining critical velocity with use of the non-linear mechanics' methods over the linear methods related to the equivalent conicity concept.

1.1. Self-exiting vibrations in railway vehicle dynamics

The problem of hunting motion of wheelset and rail vehicle body has been absorbing attention of theoreticians and practitioners since a long time. Opinions and definitions of rail vehicle stable motion connected with hunting phenomenon have been varying significantly in the period of railway existence. Review of their progress is done by Knothe and Böhm (1999). Further on, we shall refer to the selected elements of that publication. We mean those important in connection with the present article.

Explanation of hunting motion was of purely kinematical character at the beginning. Force interactions were disregarded completely. The phenomenon was explained with geometry of two conical wheels united with a common axle. Next, an important change came thanks to appearance of the rolling contact theory and its application to wheel/rail system. Henceforth the friction forces in wheel/rail contact became known. This enabled to take account of influence of all forces and torques acting on a wheelset and it became possible to

explain the phenomena with the dynamics' methods.

In the domain of dynamics, a clear analogy was noticed between the lateral vibrations of a wheelset and the vibrations of elementary systems analysed in theory of self-exciting vibrations (e.g. Osinski, 1981). In both cases, one deals with periodic vibrations of constant amplitude which theory calls the limit cycles.

According to the definition – self-exciting vibrations are the ones originating in the system under the influence of external energy source of intensity constant in time. Three subsystems can be distinguished within the system, making self-exciting vibrations possible: source of energy, energy control valve, and vibrating system. The following pairs correspond to these elements in a moving rail vehicle: source of energy – traction (the engine changing fuel energy or electricity into energy of motion, while in the simulation it can be the assumption of constant velocity of motion); energy control valve – contact forces between wheel and rail; vibrating system – vehicle on track. There is a feedback between vibrating system and energy control valve, which enables to stabilise the energy flow.

Characteristic feature of the self-exciting vibrations is that after enough duration, they become the periodic vibrations (limit cycles). The single limit cycle does not depend on the perturbation (initial conditions) that caused it, providing this particular cycle, but not the other, appears. In the main, vibrating system subject to the self-exciting vibrations of a given amplitude dissipates energy (it is a damped system). If the amount of energy supplied to such a system is big enough, however smaller than the maximum amount that may be potentially dissipated, then a vibration amplitude exists at which the total energy of the system is constant during a single period. The next feature of the self-exciting systems is an existence of at least one element with its characteristic being non-linear function of the system state. Presence of such non-linear element causes that the supplied and dissipated energies within the system are equal to each other only for one value of the amplitude (in the simplest case). Both the

amplitude and the other vibration parameters can be handy as the indicators characterizing state of the system.

Let us mention next that self-exciting vibrations theory introduces the concepts of stable and unstable limit cycles (e.g. Osinski, 1981). Such cycles occur alternately one after another and this can happen again and again. In this case one talks about multiple periodic solutions. Generally solutions tend to the stable cycles and move away from the unstable ones. It depends on range of the initial amplitude (range of the initial conditions) which particular stable cycle is taken by system as the solution. Besides, the cycles of soft and hard excitations are referred to. In the first case, just minimum amount of the supplied energy is necessary to initiate the self-exciting vibrations. In the second case, except that condition, the additional one exists, namely some minimum values of initial conditions are necessary to initiate the vibrations.

Almost all features described above, typical for self-exciting vibrations can be confirmed through simulation methods in case of wheelset vibrations. In fact, these results are not formal mathematical proof of limit cycles existence. However, without bigger doubts they confirm possibility to apply the self-exciting vibrations theory to explanation of wheelsets oscillations. The example of investigations focused on the demonstration of limit cycle existence are those described by Zboinski and Dusza (2002) and Dusza (2005). They confirmed the typical limit cycle's properties in case of wheelset hunting motion: requirement for some minimum amount of the energy necessary to initiate the self-exciting vibrations, as well as the cycle amplitude's independence of initial conditions. First of the mentioned properties means in practice a minimum velocity (critical velocity) above which the limit cycle appears. It was also demonstrated that limit cycle of the investigated wheelset was that one of hard excitation. It means that despite the critical velocity was reached, the initial conditions exceeding certain minimum value were also necessary to initiate the cycle. The

property that was not confirmed in the discussed studies was the multiple and alternating occurrence of stable and unstable limit cycles. For big oscillation amplitudes it could be explained by interaction between wheel flange and rail, which causes dramatic change of the system properties.

On the other hand there are works that show or report that multiple solutions are possible in case of wheelset oscillations (e.g. Gasch at al., 1984; Goodal and Iwnicki; 2004; Hoffmann, 2006). It might be stated with the small risk that worn rails caused multiple periodic solutions in the work by Gasch at al. (1984). Concluding, despite particular limit cycle does not depend on the initial conditions, general solution of the system depends on them in case of the co-existing multiple solutions.

1.2. Analysis of non-linear lateral stability of rail vehicles based on bifurcation plots

Interpretation of wheelset's hunting motion obtained on the grounds of self-exciting vibrations theory was completed and extended by including in the considerations the achievements of bifurcation theory. Thanks to this, it became possible to distinguish and explain different values of linear v_c and non-linear v_n critical velocities. The explanation is Hopf's bifurcation, typical as it appeared in the wheelset-track system. As shown, e.g. in reference by Xu at al. (1992), in the case of subcritical bifurcation of that kind $v_n < v_c$, whereas in the case of supercritical situation both velocities coincide, thus $v_n = v_c$. Utilisation of the bifurcation theory resulted in the transfer of stability analysis of wheelset motion to so-called bifurcation plots.

Analysis of bifurcation plots is a fundamental issue in contemporary stability analysis of rail vehicles (Huilgol, 1978; Kass-Petersen and True 1983, 1984; and eventually survey by Knothe and Böhm, 1999). Such analysis makes it possible to determine position of regions of stable and unstable stationary, as well as stable and unstable periodic solutions in relation to each other. It is also well suited to representation of the multiple periodic solutions.

The shape of bifurcation plot that is representative for some non-linear properties of railway vehicles is shown in Fig. 1 (Moelle and Gash, 1982; Xu at al., 1992; Knothe and Böhm, 1999; Schupp, 2004; Polach, 2006). Note existence of just one line representing stable periodic solutions for the situation shown in Fig. 1. Despite relatively wide range of validity of Fig. 1, it does not represent the general case. Examples of other forms of bifurcation plots for railway vehicle, including multiple periodic solutions, can be found e.g. in the works by Moelle and Gasch (1982), Gasch at al. (1984), True (1992), True and Jensen (1994-a) and Hoffmann (2006). Terminal point of the line representing stable periodic solutions in Fig. 1 determines velocity v_s. It is velocity at which the calculations are stopped for any reason. It could be an arbitrary stop or stop due to unbounded growth of oscillations. Velocity corresponding to the terminal point in view, was called in earlier works as the derailment velocity (e.g. Moelle and Gasch, 1982), and sometimes denoted with v_d. The use of this term is questionable in the simulation studies, considering limited possibility of derailment projection by simulation programmes. There is also another difference between Fig. 1 and bifurcation plots from the earlier works. It is the line, placed above the line for stable periodic solutions (as e.g. that in Fig. 1), representing unstable periodic solutions (e.g. Moelle and Gasch, 1982). This line is absent in Fig. 1. Although non-linear dynamics tells that such line must be there, demonstration of its existence for big lateral displacements of wheelset is difficult (if not impossible). Note that the theory rather does not take account of dramatic change in the system properties, as those occurring for big lateral displacements of wheelset. They are caused by wheel flange contacting with rail head in such conditions. On the other hand, additional lines for the unstable periodic solutions can be seen on the bifurcation plots representing rail vehicle systems with multiple (periodic) solutions. Then however wheelset's oscillations are of smaller amplitudes and flange contact does not occur.

The analysis based on bifurcation plots became possible thanks to wide spread of

simulation techniques and achievement of high effectiveness by them. It enabled to create more and more advanced mathematical models and this way more precise description of the phenomena taking place in a real object. In most present-day studies of stability of rail vehicle motion bifurcation plots (stability plots) are first built and then analysed. When building these plots, the results of simulations of motion are utilised, with vehicles represented by their mathematical models of different complexity. In most such studies motion along a straight track is considered. Their authors focus on analysis of the lateral dynamics of vehicle, and base on analysis of the parameters that characterize vibrations (self-exciting ones) of vehicle model. Example of such works might be those by Gash at al. (1984), True (1992), True and Jensen (1994-a, 1994-b), True at al. (1996), Knothe and Böhm (1999), Stichel (2002), Schupp (2004), Goodall and Iwnicki (2004), as well as Polach (2006).

Important problem in studying stability of motion is looking for critical values of bifurcation parameters (also called active parameters of the system). These are values for which a significant increase or change in type of solution of mathematical model occurs. In case of rail vehicle model the velocity of motion v is such a parameter. Influence of this parameter on the system properties is actually illustrated on bifurcation plot (Fig. 1). For velocities smaller than critical value, denoted with v_n, one always obtains stable stationary solutions ($y_{lw} = 0$). In the moment of occurrence of velocity v_n (and above v_n), a sudden change of solution character can happen from stable stationary to stable periodic one (solid line for both types of stable solutions is used in Fig. 1). Such change corresponds to appearance of self-exciting vibrations in the system. For the systems of hard excitation, the necessary condition for such appearance is presence of sufficiently big initial conditions. Just described phenomenon is related to occurrence of subcritical Hopf's bifurcation indicated in Fig. 1. In case of the system with subcritical properties (as shown in Fig. 1), bifurcation of the stable stationary solution into unstable stationary and unstable periodic solutions happens.

Since solutions move away from the unstable (periodic) solution and tend to the stable solutions, so under sufficiently large perturbation (initial conditions), they are attracted by the stable periodic solution. For smaller perturbations, they are attracted by the stable stationary solution, as long as $v_n<v<v_c$. For the systems of soft excitation, the bifurcation is of supercritical character (e.g. Xu at al., 1992). Then $v_n = v_c$ and no line representing unstable periodic solutions exists.

Reaching the critical value of active parameter by system does not mean a loss of the stability. It happens so, as the newly created periodic solution lasts for freely long time (here on the freely long distance of simulation). Besides, one can note in Fig. 1 that periodic character of solutions is preserved with a rise of bifurcation parameter value in the supercritical zone (i.e. for $v>v_c$). The situation changes when active parameter reaches value v_s (Fig. 1). Then, unbounded growth of the oscillations occurs resulting in stoppage of the calculations. Such growth is sometimes quite sudden. Sometimes however, the periodic character of the solution is lost first. The amplitude and frequency change slowly and also it is not the stationary solution. Concluding, some symptoms of unstable motion can be observed prior to the unbounded growth. The point in Fig. 1, denoted with symbol v_c indicates the value of critical velocity for a linear system (e.g. Moelle and Gasch, 1982, and Schupp, 2004).

The search of critical value for bifurcation parameter, and the character and value of the solutions for entire scope of bifurcation parameter changes, makes a subject for stability studies of non-linear systems. In particular, for rail vehicles, it most frequently corresponds to values of critical velocity v_n, as well as to the character and fluctuations in lateral displacements of wheelsets below and above v_n, up to v_s.

Finally, it is should be stressed that chaotic solutions (e.g. Verhulst, 1990) can appear in the rail vehicle-track system, as shown mainly in works by True (e.g. True, 1992; True and Jensen, 1994-a, 1994-b; Jensen and True, 1997; Hoffmann, 2006; Hoffmann and True, 2008;),

but also in works by others (e.g. Stichel, 2002; Zboinski and Dusza, 2006). The non-linearities in vehicle suspension system (dry friction, bump stops, clearances and so on) seem to intensify their appearance. The works cited above show that the method of studying the dynamical properties on the basis of bifurcation plots suits excellently to the analysis of such systems.

2. The model being investigated

Simulation studies within this article were performed utilising the modelling method, mathematical model, and simulation software applied in the earlier works. Therefore we confine the information on this topic. Mathematical model of the system was built in accordance with the generalised methodology of modelling for railway vehicle dynamics (Zboinski, 1999, 2001, 2004). Dynamics of vehicle in this method is the dynamics of relative motion. It means the description in relation to the reference systems that are moving along track centre line. In the description, Lagrange formalism of type II was applied but adapted to the description in moving reference frames, (Zboinski, 1999; Kisilowski and Knothe (Eds.), 1991). Consequently, 2nd-order ordinary differential equations describe motion of the mechanical system.

The most comprehensive specification of the mathematical model, and of the corresponding simulation software can be found in the work by Zboinski (1998). Nevertheless, also other references (Zboinski, 1999, 2004; Zboinski and Dusza, 2002, 2004-a, 2006) can be helpful. Here, let us remind you that it is a model of the two-axle non-traction rail vehicle, with primary suspension only, of structure given in Fig. 2(c). It has got its real counterpart within British railways rolling stock. It is HSFV1 freight car. The car model is supplemented with laterally and vertically flexible track model, of the structures shown in Fig. 2(a) and Fig. 2(b). Track model represents a standard European track with 1435mm gauge, 1:40 rail inclination, and with no geometrical irregularities. Vehicle and track models

form the discrete vehicle-track system of 18 degrees of freedom. The values of vehicle and track models' parameters can be found in Table 1 (one can see also Zboinski, 1998, 1999).

Kinematical non-linearities (Zboinski, 1999), imaginary forces of inertia (Zboinski, 1999, 2001) arising from description in moving reference systems, non-linear geometry in wheel/rail contact, as well as the non-linear tangential contact forces calculated with the use of FASTSIM programme (Kalker, 1982) constitute the non-linearities in the system.

Wheel and rail profiles with the real nominal shape (one of reasons of the non-linear geometry of contact) were applied in the model. Information about the geometry is introduced into the model through contact parameter tables. They are created with the use of RSGEO programme by Kik (1992), which is distributed by ArgeCare. The input data in this programme are Cartesian co-ordinates of wheel and rail profiles (either theoretical or measured). After smoothing this data with RSPROF subroutine, the RSGEO procedure solves two-dimensional geometrical problem, consisting in searching for position of contact points between the profiles as a function of their lateral relative shift $y_{rel}=y-y_t$ (see Fig. 2(a)). Next, the corresponding parameters are calculated and tabulated as a function of y_{rel}. In addition, variation in contact parameters coming out from wheelset yaw rotation (variable angle of attack ψ) is taken into account. This is done by generating several tables for selected range of ψ. Contact parameters are linearly interpolated relative to both the y_{rel} and the ψ. Account is taken of wheelset roll rotation ϕ through the geometrical constraint between y and ϕ. Most of the results presented in this paper were obtained for wheel/rail pair of S1002/UIC60 type being a standard in Europe. Only results shown in Section 6 refer to the Russian pair of SZDwheel/R65 type.

3. Phenomenon studies of the appearance and duration of self-exciting vibrations

Simulation studies relating to the self-exciting vibrations phenomenon started with the

straight track case that is better examined one. At the same time, the authors treated the straight track as a special case of the circular curve of infinite radius $R = \infty$. Next, our studies covered the whole range of curve radii, from the large ones R = 10000 m down to the small ones R = (300) 600 m. Investigations for particular radii R started from small velocities v. Each simulation of motion was realised with the constant velocity v. Taking into account that all system parameters remain constant during simulation, velocity v is the only parameter characterising the amount of energy being supplied into the system. The observed quantity is leading wheelset's lateral displacement y_{lw}.

Before we shall proceed to presenting and discussing example simulation results some introductory considerations are necessary. Let us realise that the problem of looking for saddle-node bifurcation (see Fig. 1) that determines critical velocity v_n (being the minimum v to start self-exciting vibrations) can be formulated in two different ways. First is the formulation as a stability problem for the periodic solution (limit cycle). Second is the formulation as a problem of existence of multiple solutions. Authors of present paper take advantage of both formulations. In fact the simplified procedure being the combination of both formulations was used.

In case of the first formulation three approaches could be exploited. The first needs sweeping over a range of initial conditions and check if despite their different values the same solution is obtained for the velocity selected. This approach matches closely mathematical definition of the stability. Variation of over the velocity v around v_n is obviously also necessary. The next options are two different methods for precise v_n determination. These are the ramping method based on continuous decrease of velocity during the single simulation (e.g. Schupp, 2004 and Hoffmann and True, 2008) or the method based on series of simulations for decreasing velocities, where results of preceding simulation are used as initial conditions in the current one.

The authors used first of the approaches mentioned above. Some simplifications were applied, however. At first, this approach was used just in the initial stage of the investigations. Next, the procedure was limited to selected radii R. These were R=600, 2000, 6000 m and ∞ (i.e. ST). Also, variation over v was limited, namely realised with 3-4 m/s interval. Such procedure was used mainly in order to be sure that real limit cycle was obtained and no multiple periodic solutions existed. As a consequence slightly overestimated values of v_n could sometimes be obtained. Nevertheless, possible inaccuracy in velocity v_n, not bigger than 4 m/s, was accepted. Example of formal stability study corresponding to the first formulation, for ST and selected velocity, is shown in Fig. 3.

In the case shown in Fig. 3 initial conditions were imposed on lateral displacements (y_{lw}, y_{tw}) of both wheelsets. Here, the limit cycles are obtained only for the initial conditions bigger than 0.004 m. For the smaller ones stable stationary solutions are obtained (vibrations decay). Thus, it can be concluded that the limit cycle we deal with in Fig. 3 is that of hard excitation. This means also that subcritical Hopf's bifurcation exists in case of the investigated system. Similar results for the selected curve radii (specified above) were obtained, too.

Preview of all results of this type allowed to know common properties of the analysed vehicle-track system for the range of radii R. Based on such knowledge a decision was taken with care to choose one set of the initial conditions for the rest of radii, despite it could result in approximate values of v_n for them. The expected inaccuracies should rather not exceed 4 m/s. The above decision was taken with serious thought, but in the main in order to speed up the calculations. Note that thanks to it just variation over the velocity was possible in the next simulations. That is why simulation results in the next subsections refer just to this set. Note also that in fact switch to the second formulation while looking for v_n value (saddle-node bifurcation) was realised in this way. The reason for such switch are primary objectives of our

studies, which needed faster calculations. The objectives themselves are presented further on.

3.1. Motion along straight track

In accordance with the foregoing considerations, the simulation results are in a form of plots representing the dependence of leading wheelset's lateral displacement y_{lw} upon distance. Results in Fig. 4 were achieved for velocities of motion equal 20, 25, and 30 m/s, respectively. In each case, the initial conditions were imposed on both wheelsets, i.e. $y_{lw}(0) = y_{tw}(0) = 0{,}0045$ m. Under these conditions, the wheelset displaced from the centre position (track centre line) returns to it (to the balance $y_{lw} = 0$) after some time. With increase of velocity v, the vibration amplitudes increase for the same distance, and also there is an elongation of distance on which the vibrations disappear (the balance is reached). Disappearance of vibrations means that amount of energy being supplied to the system is smaller than the amount of energy dissipated there. Under such circumstances, there is no chance for the self-exciting vibrations not to decay. One can state than, that the motion of vehicle is the stable stationary one within here discussed range of velocity.

Increasing still the velocity of motion (the amount of energy supplied to the system), the distance elongates again, necessary for the vibrations to disappear (Fig. 5(a)). At certain velocity (here 40 m/s), the lateral displacements y_{lw} take form that makes it impossible to state univocally, at the standard distance of simulation, whether they increase or decrease (Fig. 5(b)). Theoretically, vibrations can either disappear or develop into limit cycle (constant amplitude). Range of velocities with the behaviour like in Fig. 5(b) was however very narrow. In such situations, simulations for a longer distance (order of magnitude of a few thousands m) can give the answer. Here, vibrations tended to decay. On the other hand, the simulations for so long distances can generate doubts about their accuracy (Zboinski and Dusza, 2004-b).

Rise of velocity to 43 m/s caused the displacements reached constant value of the amplitude (and frequency) on the standard section of distance. One can state that solutions

have got character of the limit cycle being a result of self-exciting vibrations generated by the mechanical system. At this value of velocity of motion, the amount of energy being supplied to the system is equal to the amount of energy dissipated there.

Such state of the system can last for freely long time (in this instance, on a freely long distance). If one presents the results on the phase plane (Fig. 6), then one can notice that after an initial stage of motion, the trajectory describes single stable limit cycle. Width of the obtained figure arises from the account taken of transient stage before vibrations became steady.

3.2. Motion along circularly curved track

In a way analogous to straight track, the simulations were performed for motion of vehicle model in the curved track. The case study below is a circular curve of radius $\boldsymbol{R}$ = 600 m. Results in Fig. 7 represent wheelset's lateral displacements for velocities of 20, 25, and 30 m/s, respectively. As before, the initial conditions were imposed on both wheelsets, i.e. $y_{lw}(0) = y_{tw}(0) = 0{,}0045$ m.

One may observe in Fig. 7 that with increase of velocity v, there is an elongation of distance on which wheelset displaced from its balance position returns to the steady state solution (the horizontal line). The amplitudes of displacements y_{lw} increase for the same distance with increase of v, as well. Important difference comparing to the straight track is asymmetry of wheelset lateral displacement y_{lw} with respect to the track centre line (i.e. to y_{lw}=0 position). This asymmetry rises with the rise of velocity v. On the route discussed here, the superelevation of constant value h = 0,16 m was applied. This is the maximum admissible value used in practice. For the values of velocity chosen here, the superelevation deficiency occurs, being just one reason for the unsymmetrical position of wheelset in the curve. Another important reason is difference in tangential contact forces acting on the left and right wheels. It is related to the different paths to travel by the inner- and the outer wheel in the curve and

consequently to different creepages for both wheels.

Next increments in the velocity of motion (Figs. 8(a) and (b)) elongate again the distance necessary for the vibrations to disappear. This increments also increase the amplitudes of vibrations for the same distance and the asymmetry of wheelset displacement y_{lw} with respect to the track centre line. Final increment of velocity v (up to 43 m/s in Fig. 8(c)) causes that the vibrations are not of decaying character any more but take the form of steady amplitude and frequency (limit cycle). Value of v related with a jump from the stable stationary solutions to the stable periodic solutions, obtained for R=600 m, is the same as that obtained for the straight track. Similar are also such values of v obtained for rest of the radii. Thus, the conclusion can now be formulated for the investigated system. So, provided initial conditions are big enough, the radius R does not influence very much velocity v that is necessary to supply the amount of energy into the system, which is capable to initiate self-exciting vibrations. Similarly to straight track, the result exposed on phase plane (Fig. 9) creates, after an initial stage of motion, the single stable limit cycle.

Negative values of the lateral displacements y_{lw} in Fig. 7 and Fig. 8 have got a conventional character. They arise from the fact of simulating motion in the curve turning to the left. For curves turning to the right, the results are antisymmetric in relation to the horizontal axis (Ox axis) and take positive values.

3.3. Motion with velocities higher than the critical one

Accepting the assumption that stable motion of the investigated object occurs when the model describing it gives stable stationary solutions or stable periodic solutions, being the limit cycles, it seems justified to study the parameters of these cycles in the entire range of velocities they occur. Consequently, the results are presented of the succeeding simulations for straight track with velocities of 50, 55 and 65 m/s, respectively (Fig. 10).

One can see that following an increase in velocity v, the vibration amplitudes grow

slightly. At velocities 50 and 55 m/s (Figs. 10(a) and 10(b)) they still preserve the character of limit cycle. However, this situation changes at some velocity v_s (in this instance 65 m/s – Fig. 10(c)). Here, at the terminal part of the studied distance, the vibrations yet loose character of limit cycle (the amplitude and frequency change). At this velocity, our calculations yield unbounded growth in amplitude and are stopped. Two types of such growth were observed in our studies. The first corresponds to Fig. 10(c). Here, unbounded growth in the wheelset yaw angle ψ_{lw} (angle of attack) happened, while no such growth in y_{lw} was observed. For the second, direct unbounded growth in y_{lw} occurs. Samples of that type of results can be found in Dusza (2005), Zboinski and Dusza (2004-b, 2008). The behaviours as described mean that with velocity v_s, the amount of energy supplied to the system is bigger than amount of the energy dissipated there. Therefore such cases evidence the unstable motion of vehicle model. Analogous results, though shifted (i.e. asymmetrical) in relation to the horizontal axis, we obtained for the circular curves.

Two additional comments should be made in view of the previous paragraph. Firstly, we have not investigated directly the reason of the unbounded growths of oscillations. Nevertheless, results in Zboinski and Dusza (2004-b, 2008) revealed that appearance of the unbounded growth in the range of realistic velocities v and also values of v_s depend strongly on the method of wheelset's mean rolling radius r_t modelling. The differences between particular methods were so big that one can not be sure if discussed growths reflect any physical phenomena. They could also be a result of wrong r_t modelling and of wrong modelling in general.

Secondly, the difference that was discussed in subsection 1.2 between stoppage of calculations for velocity v_s, which is represented e.g. by Fig. 10(c), and the real derailment should be reminded here. In addition, under v_s we should mean any velocity at which the calculations are stopped, no matter we deal with the unbounded growth started from periodic

(or quasi-periodic), stationary (or quasi-stationary), and even chaotic solutions.

4. Employing observations of self-exciting vibrations and stationary solutions in evaluation of vehicle stability in curves

One can get bifurcation plot basing on observations of change of the system's selected variable, in particular domain, under the influence of changing value of a bifurcation parameter. Here, such observations refer to the change of wheelset lateral displacement y_{lw}, in distance domain, under the influence of changing velocity v (e.g. Figs. 4, 5, and 10). The obtained theoretical bifurcation plot for the given conditions (given curve radius R and superelevation H) could look like Fig. 11(a).

This plot is similar to that for straight track in Fig. 1. The major difference appears for stationary solutions (i.e. for $v < v_c$), because then $y_{lw} \neq 0$ in a curved track. The reasons are explained further on. Another difference concerns terminal part of the plot. Note that points in Figs. 11(a) and (b) corresponding to velocity v_s are not the terminal points for the lines of stable periodic solutions, as it happens in Fig. 1. This difference emphasises limited connection of v_s with velocity at which vehicle eventually derails in reality. Different values of v_s that could be obtained with use of different simulation programmes (different modelling) are emphasised this way, too. The reason for both are limited capabilities of the simulation programmes to simulate a derailment. That problem was already discussed in Subsections 1.2 and 3.3.

In terms of building Fig. 11(a) in practice some additional information is beneficial. The reader should realise certain possible differences in determining the lines for unstable and stable periodic solutions. In case of unstable periodic solutions (dashed line joining the attractors at velocities v_c and v_n), stability analysis in type shown in Fig. 3 must be used. Sweeping over values of the initial conditions is the absolute necessity. We mean to have the possibility of determining such results. For example, studies concluded with Fig. 3 made it

possible to determine the point on the corresponding dashed (unstable) line of the following co-ordinates: v=46 m/s, y_{lw}=0.00418 m. In case of stable periodic solutions, possessing greater practical significance, the stability analysis with a thorough variation over values of the initial conditions can also be used. On the other hand, however, the simplified and faster approach based on check of the periodic solution's existence could carefully be used, too (as explained at the beginning of Section 3). It is really an attractive alternative. Here, one or a few selected set(s) of initial conditions is(are) used, depending on the system properties. While using this approach, however, one should treat it all the time as a supplement to the stability approach. In case of any doubts or randomly (just for check) the switch to sweeping over a range of the initial conditions is recommended. Despite higher risk of omission of unexpected solutions (multiple or chaotic ones), such simplified approach can be a reasonable compromise in terms of the calculation efficiency.

Now note, that during motion of the model along perfectly straight track, in conditions when vibrations decay (Fig. 4), values of displacements y_{lw} become constant and $y_{lw} = 0$ at the same time. If motion in the similar conditions takes place along circular track, then the value of y_{lw} becomes also constant, but in the main $y_{lw} \neq 0$ (Fig. 7). It comes out from existing in curves no balance of the lateral forces acting on wheelset in its symmetrical ($y_{lw} = 0$) lateral position. If in the straight track the self-exciting vibrations exist, i.e. the observed lateral displacements y_{lw} are in type of limit cycle, then sign of displacements y_{lw} changes (Fig. 10). Change of the y_{lw} sign can also happen in circular curve (Fig. 8(c)) where limit cycle is asymmetrical. Moreover, for both the stationary and periodic solutions, the solutions (s_r) for a curve turning to right and solutions (s_l) for the curve turning to left are antisymmetric ($s_r = -s_l$) to each other, provided the same curve radius R. So, the sign of y_{lw} depends on the direction of a curve turn.

Consequently, the question comes into being what value of displacements y_{lw} should

be taken on the bifurcation plot, since maximum value of y_{lw} is not univocal. Therefore in Fig. 11(a), the maximum of absolute value of lateral displacement ($|y_{lw}|$ max) was adopted instead of maximum of the displacement (y_{lw} max) used in Fig. 1.

In order to represent the character of solutions (stationary or periodic) and give the information on asymmetry of limit cycle in a curve, additional characteristic parameter of the limit cycle needed to be introduced. Peak-to-peak value was taken, measured as a distance between succeeding peaks of vibrations, from the plots representing leading wheelset's lateral displacement y_{lw} versus distance (Fig. 11(d)). The denotation (p-t-p y_{lw}) was adopted for that parameter. Obviously, in case of stable stationary solutions its value equals zero. The observation of changes in values of (p-t-p y_{lw}) under the influence of velocity variation leads to the second, non-standard bifurcation plot (Fig. 11(b)) for given conditions of motion (given curve radius R and superelevation H). This plot is absolutely necessary to fully characterize the system in instance of the stability analysis in a curved track.

The pair of bifurcation plots in Figs. 11(a) and (b), suitable to curved track analysis, represents variation of the ($|y_{lw}|$ max) and (p-t-p y_{lw}) as a function of velocity v, for single radius R. Scheme of the method of building such a pair is shown in the whole Fig. 11. Let us explain this figure shortly. Under conditions of motion where no self-exciting vibrations (in form of limit cycle) occur, the stable stationary solutions are obtained (Fig. 11c). Steady value of the displacements read for the terminal section of the distance gives single point on the diagram of ($|y_{lw}|$ max) = f(v) - Fig. 11(a). Peak-to-peak value is equal zero, here. This gives a point that is situated on the horizontal axis of the diagram for (p-t-p y_{lw}) = f(v) - Fig. 11(b). When the motion in form of steady self-exciting vibrations occurs (Fig. 11(d)), then the maximum of absolute value of lateral displacement y_{lw} is read, what gives single point on the diagram of ($|y_{lw}|$ max) = f(v) - Fig. 11(a). The vertical distance between the succeeding peaks of y_{lw} gives single point on the diagram of (p-t-p y_{lw}) = f(v) - Fig. 11(b).

Building the pair of the complete graphs for functions $(|y_{lw}| \max) = f(v)$ and $(\text{p-t-p}\ y_{lw}) = f(v)$ needs at least a dozen or so simulations performed of the model motion, each for different velocity v but all for the same curve radius R and superelevation H.

4.1. The method of creating stability maps illustrating stability of model within the entire range of curve radii

Basically, the procedure of stability analysis in a curve is analogous to that applied for a straight track. Nevertheless, the differences should not be passed over in silence, especially in view of significant expenditure of additional work and of additional troubles that may appear. In order to visualize better the additional attention and measures caused by the stability analysis for circular curves a block diagram was elaborated (Fig. 12). This diagram does not arise from the theory. It is mainly the result of experience gathered by the authors while realising the following works: Zboinski (1998), Zboinski and Dusza (2002, 2004-a, 2004-b, 2006), and Dusza (2005). It was assumed that all measures for determination of stability regions for straight track are standard ones, e.g. like in Moelle and Gasch (1982) and Gasch at al. (1994). That is why this part was put into one block. The part being the extension of standard measures, necessary to include motion in curves in the analysis, is more detailed. Blocks related to this part should be taken into account in succession going from the top to the bottom.

Observations leading to creation of diagrams in Figs. 11(a) and 11(b) can be done for different curve radii R, obtaining this way a set of pairs of the bifurcation diagrams. Comparison of these pairs for different R from its full range makes it possible to determine the influence of radius R on stability of motion of the investigated model. Presenting all plots in type of that in Fig. 11(a) on the single diagram, and then all plots in type of that in Fig. 11(b) on the other single diagram, we get a representation of stability of motion for the model in the entire range of the radii R, including straight track. Such representations were

named stability maps by the authors (Zboinski and Dusza, 2004-a, 2006; and Dusza, 2005). Let us notice that the preparation of stability map for the entire range of curve radii needs execution of at least several dozen single simulations of motion.

5. Representation of stability of motion in the form of stability maps. Assumptions of the method

According to the idea presented above, a number of simulations were done in order to get a representation of stability for the vehicle (its model described in Section 2). These simulations were done for straight sections ST and circular curves, from small to large radii R. In each group of simulations for particular R, each single simulation was done for a different velocity v, however so as to cover the range from 5 m/s to $v_s = v_{s(R)}$. For each simulation with a given velocity, the plot was created of wheelset lateral displacements versus velocity (as e.g. Figs. 4, 5, 7, 8 and 10). From the plots of such type, the values of maximum wheelset lateral displacements and peak-to-peak values of the displacements were read off. These values exposed as the functions of velocity for entire scope of curve radii created stability map composed of Fig. 13 and Fig. 14. It gives the representation of the model stability in any conditions of motion (in terms of R values).

Each line on the map illustrates the result for route with different curve radius. Its values are specified next to the lines. Studies were started from small velocity (v=5 m/s). Solutions of the model have got stable stationary character here. In Fig. 13 it matches usually non-zero values of maximum lateral displacements (y_{lw} max) and in Fig. 14 zero peak-to-peak values (p-t-p $y_{lw} = 0$). In case of curved track and the stationary solutions, different than zero values of (y_{lw} max) are, among others, related to track superelevation. It was selected for each value of R individually, being the nominal one for critical velocity v_n. This means an excess of superelevation in all simulations with velocities smaller than v_n. For very small velocities and large radii R, it results in a change of the sign of maximum displacements y_{lw} (see Fig. 13).

Thus, for cases like those, and only for them, use of ($|y_{lw}|$ max) would be misleading. Therefore, we departed from the recommendation formulated for Fig. 11(a) to present the maximum of absolute value of the displacements ($|y_{lw}|$ max) on the first of bifurcation plots. Instead, the bifurcation plot was created for curves turning to the right as well as the maximum of the displacements (y_{lw} max) is represented in Fig. 13.

Important in Figs. 13 and 14 are the vertical lines for velocity of 43 m/s. These lines separate the range of stable stationary solutions from the range of stable periodic ones. Also, a step change in maximum values of lateral displacements and peak-to-peak values of the displacements happens here. Just mentioned velocity is the non-linear critical velocity v_n. In the range of present article, it is the smallest velocity of motion for which the self-exciting vibrations exist in the form of limit cycle. Using the way of velocity v_n determination described at the beginning of chapter 3, value of v_n appeared to be the same for all radii R (from R = 600 m to ST) in the investigated system.

The biggest wheelset's lateral displacements (y_{lw} max) occurred for the route with R=600 m, for both the stationary and the periodic solutions (Fig. 13). Generally, for periodic solutions (i.e. when $v > v_n$), the bigger the radius R, the smaller the maximum displacement (y_{lw} max) for analogous velocities v. Here, minimum value of (y_{lw} max) is reached for straight track ST. Next, peak-to-peak values (p-t-p y_{lw}) have got opposite direction of the growth for the periodic solutions. They are smallest for the route with R=600 m, and the bigger the radius R, the bigger the peak-to-peak value (p-t-p y_{lw}) for analogous velocities v. It reaches maximum for straight track ST. Terminal point of each line corresponds to the velocity v_s, for which the calculations are stopped due to unbounded growth of the oscillations, as earlier defined in Subsection 3.3. As it can be seen, velocity v_s increases with a rise of radius R. Compare for instance $v_{s(600)}$=47 m/s, $v_{s(1200)}$=57 m/s, $v_{s(3000)}$=63 m/s, and $v_{s(ST)}$=65 m/s with each other. On the routes with curve radii R < 600 m, the calculations were stopped (due to

unbounded growth of solution) for velocities smaller than the critical velocity v_n, i.e. within stationary solutions range. That is why we decided not to present these results on the plots.

Despite a significant similarity of the map composed of Fig. 13 and Fig. 14 to theoretical plots in Fig. 11(a) and Fig. 11(b), the differences exist that should be discussed now. Firstly, the maps shown here do not present lines for unstable solutions. Secondly, they do not contain the information on linear critical velocity v_c. Thirdly, non-linear critical velocity v_n is determined with numerically effective, however simplified method. Thus approximate values of v_n were obtained. Nevertheless, one can always do it more precisely by thorough variation over values of the initial conditions for all curve radii and usage of smaller velocity interval. Another possibility would be to use already mentioned different methods of v_n determination. So, the ramping method or the method based on series of simulations for decreasing velocities (where results of preceding simulation are used as initial conditions in the current one) could be utilised. Fourthly, velocities v_s indicate univocally terminal points of the lines for stable solutions. Nevertheless, these points have got some conventional character. They do not define the physical derailment of the vehicle. One can use them only as some qualitative measure of the derailment risk. In this context, eventual comparing of v_s values for different vehicles or the same vehicle with different parameters (e.g. in the suspension) seem to be sensible.

Above mentioned differences result mainly from aims of our studies and choice of the corresponding simplifying assumptions. Our aim was to elaborate a method of stability analysis in curves for the entire range of radii R, as effective as possible. Next point was to enable to treat relatively quickly as much factors that might influence stability of railway vehicles in curves as possible. Besides, some of the simplifications in the presented maps seem to have got more theoretical than practical significance. For instance, in case of system with subcritical Hopf bifurcation (as in Fig. 1), one should rather not expect that for velocities

between v_n and v_c stable stationary solutions correspond to behaviour of a real system. It comes out from properties of a real track that possess both the geometrical irregularities and the asymmetry in vertical stiffness. This is a reason of excitation in the real system. Consequently while studying the stability for $v_n<v<v_c$, one should rather expect that bigger initial conditions leading to the periodic solutions, correspond to the real conditions of motion better than smaller (or zero) ones, leading to the stationary solutions. In supercritical case (Xu at al., 1992), the problem does not exist, since then $v_n=v_c$. The step change from stationary to periodic solutions, provided no multiple periodic and chaotic solutions occur, evidence almost for sure that we deal with subcritical Hopf's bifurcation in case of the investigated model.

At this stage of the article two matters should be stressed. First is the uniform character of the model properties for all radii R (including ST), as in Figs. 13 and 14. The most distinctive here is a division of the velocity range into two parts by common critical velocity value v_n=43 m/s. These parts refer to the stable stationary and periodic solutions, correspondingly. Also dependence of (y_{lw} max) and (p-t-p y_{lw}) on radius R is uniform. It seems, at small risk of mistake, that these features result from the simple vehicle model we used. We mean simple model structure (Fig. 1), linear suspension elements and nominal (unworn) S1002/UIC60 wheel/rail profiles.

The second matter to be stressed are the consequences of just described uniform properties, for the method we applied in the present article. It should be stated, here, that earlier described simplifications in the method were possible to apply thanks to those uniform properties. Consequently, in instance of more severe non-linearities and complicated structure of the model more caution must be applied and better justified formal methods are recommended. We mean in particular: looking for the saddle-node bifurcation utilising formulation of the problem as a stability problem for periodic solution rather than as a problem of existence of multiple solutions (Section 3); alternative use of different exact

methods of velocity v_n determination; and determination of courses for unstable periodic solutions. Failure to do so may result in wrong determination of v_n, and omissions of multiple and chaotic solutions that might actually be of importance for theory or practice.

6. Sample of stability analysis – investigation into influence of the chosen factor on the stability

With use of the method presented, the studies were done for considerable number of factors on their influence on the stability. These factors were: shape of wheel and rail nominal profiles; wear of wheel and rail profiles with regard to its magnitude and place of the biggest intensity; track superelevation; parameters in vehicle suspension, including values of stiffness and damping for longitudinal, lateral and vertical directions; vehicle type (bogie, 2-axle vehicle); method of considering wheelset's angle of attack; method of determination of wheelset mean rolling radius; and rail inclination. Results of these studies were presented in Zboinski and Dusza (2002, 2004-a, 2004-b, 2006, 2008) and Dusza (2005).

From the factors mentioned above, we selected one to be presented in this article. It is the shape of wheel and rail profiles. We'll show the very spectacular influence of this factor on the corresponding stability maps. The results differ from those in the above cited references, including solutions for velocities smaller than v_n. The analysis is confined to just two pairs of profiles since first of all, we treat it as a sample of the method's potentiality. Results for the pair of wheel/rail profiles of type S1002/UIC60 are shown in Fig. 13 and Fig. 14, while for the pair of type SZDwheel/R65 in Fig. 15 and Fig. 16.

Stability analyses that exploit stability maps proposed by the authors are performed mainly from the point of view of four elements. First two are value of critical velocity v_n and value of velocity v_s. The next two are the courses versus velocity v of - the maximum of absolute value of lateral displacement y_{lw} ($|y_{lw}|$ max) or alternatively the maximum of this displacement (y_{lw} max), - and the peak-to-peak value of displacement y_{lw} (p-t-p y_{lw}).

Critical velocity v_n for the first pair is significantly higher (43 m/s) than for the second pair (25 m/s). Velocities v_s on all routes (read for all curve radii, including $R = \infty$) in case of the first pair are considerably lower than for the second pair. It can be seen while comparing values of $v_{s(600)}$, $v_{s(1200)}$, $v_{s(3000)}$, and $v_{s(ST)}$ in Figs. 13 and 14 with the corresponding values in Figs. 15 and 16. For both pairs, the biggest values of this velocity happen for straight track ($v_{s(ST)}$) and equal 65 and 130 m/s, respectively.

The course of (y_{lw} max) below the critical velocity is qualitatively similar for both pairs. In terms of magnitude, the displacements are bigger for the second pair of profiles. Track superelevation for both pairs was chosen as a constant for each of the radii R and having nominal value for velocity $v = 43$ m/s, being the critical velocity for model equipped with the first pair. Values of (y_{lw} max) for S1002/UIC60 pair are bigger in general, and also for the same velocities, than values of ($|y_{lw}|$ max) for SZDwheel/R65 pair. Important difference makes the boundary value of curve radius R below which the limit cycle does not appear above critical velocity v_n. In case of the standard European pair, there is no such value. It means that exceeding v_n results in appearance of the limit cycles for all values of R. The exception are those radii only ($R < 600$ m) for which v_s (calculations stop) is reached prior to v_n. In case of the Russian pair this boundary value is approximately $R = 2150$ m. This means that for curves with radii $R < 2150$ m, there are no limit cycles at all, also after v_n is exceeded.

Peak-to-peak values (p-t-p y_{lw}) for both pairs are the very biggest for straight track ST. Qualitative differences for this quantity in case of both pairs of profiles are visible. In the main they appear for $R < \infty$. However, they become spectacular for $R < 2150$ m, what is connected with absence of limit cycles for such R in case of the second pair (Fig. 16). Values of (p-t-p y_{lw}) for the second pair are visibly smaller than for the fist one, in general.

In consequence of just described differences between both pairs of profiles, we can formulate the following recommendations and conclusions for the railway practice. The

second pair of profiles gives stationary solutions below v = 25 m/s, i.e. about 90 km/h. So, it is more suitable for freight rather than for passenger cars that run with high and very high speeds. The first pair gives stationary solutions below v = 43 m/s, i.e. about 155 km/h, thus it is much better suited for passenger cars than the previous one. When in the range of self-exciting vibrations (limit cycles), the second pair has better properties in terms of ride quality than the first pair (smaller maximum and peak-to-peak values of the displacements y_{lw}). Despite very limited connection of v_s with a real derailment, much higher values of v_s for the second pair cannot be passed over in silence. Although, it is not proven, it seems that smaller risk of the derailment could be concluded for the SZDwheel/R65 pair comparing to the S1002/UIC60 pair. On the other hand, it should be emphasised that nominal profile of S1002 wheel is derived from the profile shapes we obtain as a result of wear process. Wheel profile used by SZD railways is closer to the conical profile (than S1002 profile) and that is why it can take different shape(s), caused by its wear during operation. It will obviously result in a change of the vehicle dynamical properties, maybe towards properties for the S1002 profile. Independently of these considerations, another fact should be stressed. Namely, parameters of vehicle suspension affect the dynamical properties significantly, and in particular the value of v_n. Thus, intentional change of these parameters, or of the suspension construction, may improve the dynamical properties of vehicle for both pairs of the profiles.

7. Conclusion

The basic idea of determining areas of stable and unstable solutions of railway vehicle models in a curved track was presented in the present article. Strong reference to physical aspects of the problem was made at the same time. Here, the fundamental importance of self-exciting vibrations was indicated. Next, the importance and validity was shown of Hopf's and saddle-node bifurcations in curved track analysis, just like it is in straight track case.

Thanks to the simple model used in the simulations, it became possible to explain the

place and usefulness of the basic knowledge on the self-exciting vibrations and the bifurcations mentioned in the railway vehicle stability analysis in a curved track. The procedure (method) to determine the stable stationary and periodic solutions in a curved track was also presented. The simplicity of the model resulted in absence of phenomena of unexpected multiple and chaotic solutions in our results. Thanks to it, we could simplify the procedure vastly. The benefits are faster calculations and consequently more factors investigated that influence stability in a curved track. In general case, however, there is a risk of omitting some multiple and chaotic solutions and to determine critical velocity incorrectly. That is why authors of the present paper do not consider their procedures as absolutely recommended. They advise to utilise as much as possible from their approach, being very careful at the same time. In the general case or in the case of particular vehicle of more sophisticated structure (e.g. 4-axle, bogie vehicle) or strong non-linearities (e.g. dry friction in the suspension or worn wheel/rail profiles) more formal approach is unavoidable. For instance formal stability study rather than looking for multiple solutions in determining saddle-node bifurcation is more reliable. Comparing to what the authors did in this paper the following three elements should be supplemented. First, all radii R should be covered by the stability analysis (instead of just the selected ones). Second, such analysis should be performed for velocities at smaller interval (about 1 m/s instead of 3-4 m/s). Third, whole velocity range should be treated in that way (instead of mainly the range around v_n).

Study on stability of rail vehicle model utilising observation of the system quantities that change with appearance of self-exciting vibrations is recently the basic and effective research method for multi-dimensional systems of such kind (Knothe and Böhm, 1999). This method enables to determine precisely the critical value of active parameter as well as analyse the model properties in subcritical and supercritical zones of the parameter value. This is the essence of utilisation of the method in practice. Motion with velocities higher than critical one

is not desired during vehicle operation. It is obvious that appearance of the hunting in the real system is definitely worse that its absence. It results in: worse running quality, bigger wear in rail/wheel system, raised derailment risk, and faster degradation of the track. Despite that, the motion in such conditions does not mean an absolutely unacceptable situation (e.g. in terms of safety). Therefore, knowledge about solutions (behaviour) in this velocity range is not less interesting than for the smaller velocities. Besides, note that such situation can happen in reality in case of motion with the excessive velocity (above the admissible one). Let us take the entrance into curve of small radius as an example, where admissible velocity is distinctly smaller than in the straight section. In such instance, knowledge about the width of range of stable periodic solutions (i.e. interval between v_n and v_s) provides the information on the safety margin between achievement of critical value of velocity and stability loss, resulting in loss of faith in the results of numerical simulations.

The authors succeeded to demonstrate that their approach can be applied well to the circular sections of track. The method used by them appeared to be efficient and reliable, as shown in numerous studies on influence of different factors on the stability of motion. The results obtained show the sense of stability analysis in curved track and its practical aspects which are sometimes questioned. Original in the method is creation of stability maps being in fact a kind of the bifurcation plots. The maps do not restrict themselves to results of stability analysis for single curves of a certain radius R. They also expose representation of model's stability for the entire range of curve radii, and straight track as well. The authors express their hope that this paper will contribute to widening the circle of people of opinions conformable to theirs on the stability of rail vehicles in general, and on the stability in curved track in particular.

Literature:

Dukkipati, R.V., 1994. Modelling and simulation of the hunting of a three-piece railway truck

on NCR curved track simulator, in: Shen, Z. (Ed.), Proc. 13th IAVSD Symp. on The Dynamics of Vehicles on Roads and on Tracks. Vehicle Syst. Dyn. 23(suppl.), 105-115.

Dusza, M., 2005. Simulation studies of railway vehicle motion stability in curves with regard to influence of changes of the system chosen parameters. PhD thesis, Warsaw Technical University, Faculty of Transport, Warsaw (in Polish).

Elkins, J.A., 1992. Prediction of wheel/rail interaction: the state-of-the-art, in: Sauvage, G. (Ed.), Proc. 12th IAVSD Symp. on The Dynamics of Vehicles on Roads and on Tracks. Vehicle Syst. Dyn. 20(suppl.), 1-27.

Gasch, R., Moelle, D., Knothe, K., 1984. The effect of non-linearities on the limit-cycles of railway vehicles, in: Hedrick, K. (Ed.), Proc. 8th IAVSD Symposium, Cambridge, USA. Swets & Zeitlinger, Lisse, pp. 207-224.

Goodall, R.M., Iwnicki, S.D., 2004. Non-linear dynamic techniques v. equivalent conicity methods for rail vehicle stability assessment, in: Abe, M. (Ed.), Proc. 18th IAVSD Symp. on The Dynamics of Vehicles on Roads and on Tracks. Vehicle Syst. Dyn. 41(suppl.), 791-799.

Hoffmann, M., 2006. Dynamics of European two-axle freight wagons. PhD thesis, Technical University of Denmark, Informatics and Mathematical Modelling, Lyngby.

Hoffmann, M., True, H., 2008. The dynamics of European two-axle railway freight wagons with UIC standard suspension, Proc. 20th IAVSD Symp. on The Dynamics of Vehicles on Roads and on Tracks. Vehicle Syst. Dyn. vol. 46 (s1), pp. 225-236.

Huilgol, R.R., 1978. Hopf-Friedrichs bifurcation and the hunting of a railway axle. Quart. J. of Appl. Math. 36, 85-94.

Jensen, C.N., True, H., 1997. On the new route to chaos in railway dynamics. Nonlinear Dynam. 13, 117-129.

Kalker, J.J., 1982. A fast algorithm for the simplified theory of rolling contact. Vehicle Syst. Dyn. 11, 1-13.

Kass-Petersen, C., True, H., 1983. A bifurcation analysis of nonlinear oscillations in railway vehicles. Vehicle System Dynamics, 12, 2-3.

Kass-Petersen, C., True, H., 1984. A bifurcation analysis of nonlinear oscillations in railway vehicles. Vehicle System Dynamics, 13, 655-665.

Kik, W., 1992. Comparison of the behaviour of different wheelset-track models, in: Sauvage, G. (Ed.), Proc. 12th IAVSD Symp. on The Dynamics of Vehicles on Roads and on Tracks. Vehicle Syst. Dyn. 20(suppl.), 325-339.

Kisilowski, J., Knothe, K. (Eds.), 1991. Advanced Railway Vehicle System Dynamics. WNT,

Warsaw.

Knothe, K., Böhm, F., 1999. History of Stability of Railway and Road Vehicles. Vehicle Syst. Dyn. 31, 283-323.

Lee, S.Y., Cheng, Y.C., 2003. Nonlinear hunting stability analysis of high-speed railway vehicles on curved tracks, Heavy Veh. Syst. 10(4), 344-361.

Lee, S.Y., Cheng, Y.C., 2005. Nonlinear analysis on hunting stability for high-speed railway vehicle truck on curved tracks, J. Vib. Acoust. – Trans. ASME, 127(4), 324-332.

Lee, S.Y., Cheng, Y.C., 2006-a. Hunting stability analysis of a new dynamic model of high-speed railway vehicle moving on curved tracks, in: Proc. 15th IASTED International Conference on Applied Simulation and Modelling vol.2006, art. 522-055, pp. 8-14.

Lee, S.Y., Cheng, Y.C., 2006-b. Influences of the vertical and roll motions of frames on the hunting stability of trucks moving on curved tracks. J. Sound Vib. 294(3), 441-453.

Lee, S.Y., Cheng, Y.C., Kuo, C.M., 2005. Non-linear modelling and analysis on the hunting stability of trucks moving on curved tracks, in: Proc. 14th IASTED International Conference on Applied Simulation and Modelling vol.2005, art. 469-804, pp. 422-426.

Moelle, D., Gasch, R., 1982. Nonlinear bogie hunting, in: Wickens, A. (Ed.), Proc. 7th IAVSD Symposium, Cambridge, UK. Swets & Zeitlinger, Lisse, pp. 455-467.

Osinski, Z., 1981. Theory of oscillations, PWN, Warsaw (in Polish).

Polach, O., 2006. On non-linear methods of bogie stability assessment using computer simulations. P. I. Mech. Eng. F – J. Rail Rapid Transit 220(1), 13-27.

Schupp, G., 2004. Computational bifurcation analysis of mechanical systems with applications to Railway vehicles, in: Abe, M. (Ed.), Proc. 18th IAVSD Symp. on The Dynamics of Vehicles on Roads and on Tracks. Vehicle Syst. Dyn. 41(suppl.), 458-467.

Shen, Z., 1992. On principles and methods to reduce the wheel/rail forces for rail freight vehicles, in: Sauvage, G. (Ed.), Proc. 12th IAVSD Symp. on The Dynamics of Vehicles on Roads and on Tracks. Vehicle Syst. Dyn. 20(suppl.), 584-595.

Stichel, S., 2002. Limit cycle behavior and chaotic motions of two-axle freight wagons with friction damping. Multibody Syst. Dyn. 8, 243-255.

True, H., 1992. Railway vehicle chaos and asymmetric hunting, in: Sauvage, G. (Ed.), Proc. 12th IAVSD Symp. on The Dynamics of Vehicles on Roads and on Tracks. Vehicle Syst. Dyn. 20(suppl.), 625-637.

True, H., 1994. Does a critical speed for railroad vehicles exists?, in: Proc. ASME/IEEE/AREA Joint Railroad Conference, pp. 125-131.

True, H., 1999. On the theory of nonlinear dynamics and its applications in vehicle systems

dynamics. Vehicle Syst. Dyn. 31, 393-421.

True, H., 2006. Recent advances in the fundamental understanding of railway vehicle dynamics, Int. J. Vehicle Des. 40(1/2/3), 251-264.

True, H., Birkedal Nielsen, J., 1998. in: On the Dynamics ofSteady Curving of Railway Vehicles, in: Zobory, I. (Ed), Proc. 6th Mini Conference on Vehicles System Dynamics, Identification and Anomalies, Technical University of Budapest, pp. 73-81.

True, H., Hansen, T.G., Lundell H., 2005. On the Quasi-Stationary Curving Dynamics of a Railroad Truck, Proc. ASME/IEEE/AREA Joint Railroad Conference, ASME-RTD 29, 131-138.

True, H., Jensen, J.Ch., 1994-a. Parameter study of hunting and chaos in railway vehicle dynamics, in: Shen, Z. (Ed.), Proc. 13th IAVSD Symp. on The Dynamics of Vehicles on Roads and on Tracks. Vehicle Syst. Dyn. 23(suppl.), 508-520.

True, H., Jensen, J.Ch., 1994-b. Chaos and asymmetry in Railway vehicle dynamics. Periodica Polytechnica Ser. Transp. Eng., 22(1), 55-68.

True, H., Jensen, J.Ch., Slivsgaard E., 1996. Non-linear Railway Dynamics and Chaos, in: Zobory, I. (Ed), Proc. 5th Mini Conference on Vehicles System Dynamics, Identification and Anomalies, Technical University of Budapest, pp. 51-60.

Verhulst, F., 1990. Nonlinear differential equations and dynamical systems, Springer-Verlag, Berlin, Heidelberg, New York….

Wickens, A.H., 1965-a. The dynamics of railway vehicles on straight track: fundamental consideration of lateral stability. P. I. Mech. Eng. F - J. Rail Rapid Transit 180(3), 1-16.

Wickens, A.H., 1965-b. The Dynamics Stability of a simplified four-wheeled vehicle having profiled wheels. Int. J. Solids Structs 1, 385-406.

Xu, G., Steindl, A., Troger, H., 1992. Nonlinear stability analysis of a bogie of a low-platform wagon, in: Sauvage, G. (Ed.), Proc. 12th IAVSD Symp. on The Dynamics of Vehicles on Roads and on Tracks. Vehicle Syst. Dyn. 20(suppl.), 653-665.

Zboinski, K., 1998. Dynamical investigation of railway vehicles on a curved track, Eur. J. Mech. A-Solids 17(6), 1001-1020.

Zboinski, K., 1999. Importance of imaginary forces and kinematic type non-linearities for description of railway vehicle dynamics, P. I. Mech. Eng. F – J. Rail Rapid Transit 213(3), 199-210.

Zboinski, K., 2001. Relative kinematics exploited in Kane`s approach to describe multibody systems in relative motion, Acta Mech. 147, 19-34.

Zboiński K., 2004 Numerical and traditional modelling of dynamics of multi-body system in

type of a railway vehicle, *Archives of Transport*, 16(3), 81-106.

Zboinski, K., Dusza, M., 2002. Simulation investigation of railway vehicle dynamics in curved track, in: Proc. XV Scientific-Technological Conference Rail-Vehicles 2, pp. 343-352 (in Polish).

Zboinski, K., Dusza, M., 2004-a. Analysis and method of the analysis of non-linear lateral stability of railway vehicles in curved track, in: Abe, M. (Ed.), Proc. 18th IAVSD Symp. on The Dynamics of Vehicles on Roads and on Tracks. Vehicle Syst. Dyn. 41(suppl.), 222-231,

Zboinski, K., Dusza, M., 2004-b. On the problems with determination of railway vehicle lateral stability in curves by means of numerical simulation, in: Proc. 9th Mini Conference on Vehicle System Dynamics, Identification and Anomalies. Budapest University of Technology and Economics, Budapest, pp. 163-170.

Zboinski, K., Dusza, M., 2006. Development of the method and analysis for non-linear lateral stability of railway vehicles in curved track, in: Bruni, S., Mastinu, G. (Eds.), Proc. 19th IAVSD Symp. on The Dynamics of Vehicles on Roads and on Tracks. Vehicle Syst. Dyn. 44(suppl.), 147-157.

Zboiński, K., Dusza, M., 2008. Bifurcation approach in studying the influence of rolling radius modelling and rail inclination on the stability of railway vehicles in a curved track, Proc. 20th IAVSD Symp. on The Dynamics of Vehicles on Roads and on Tracks. Vehicle Syst. Dyn. vol. 46 (s1), pp. 1023-1037.

Zeng J., Wu P., Stability analysis of high-speed railway vehicles, JSME International Journal Series C, Mechanical Systems, Machine Elements and Manufacturing, vol. 47 (2) (special issue), pp. 464-470, 2004.

Zeng, J., Wu, P., 2005. Stability of high-speed train, J. Traffic and Transportation Engineering 5(2), 1-4.

Fig. 1. Shape of bifurcation plot, typical for rail vehicle in a straight track ST

Fig. 2. Nominal model structures of: (a) – track laterally, (b) – track vertically, (c) – vehicle

Fig. 3. Influence of the initial conditions on limit cycle amplitude and general solution of the system. Motion along ST with velocity v=46 m/s (critical velocity v_n=43 m/s at the same time)

Fig. 4. Leading wheelset lateral displacements y_{lw} versus distance for straight track and velocities of 20, 25, and 30 m/s

Fig. 5. Leading wheelset lateral displacements y_{lw} versus distance for straight track and velocities of 35, 40, and 43 m/s

Fig. 6. Lateral displacement y_{lw} and its time derivative for velocity of 43 m/s and straight track on phase plane

Fig. 7. Leading wheelset lateral displacements y_{lw} versus distance for curved track of R=600 m and for velocities of 20, 25, and 30 m/s

Fig. 8. Leading wheelset lateral displacements y_{lw} versus distance for curved track of R=600 m and for velocities of 35, 40, and 43 m/s

Fig. 9. Lateral displacement y_{lw} and its time derivative for velocity of 43 m/s and circularly curved track of R=600 m on phase plane

Fig. 10. Leading wheelset lateral displacements y_{lw} versus distance for straight track and velocities of 50, 55 and 65 m/s

Fig. 11. The scheme of creating a pair of the bifurcation plots for stability analysis in circularly curved track

Fig. 12. Block diagram of the method's extension to the curved track analysis

Fig. 13. Part one of stability map – maximum of leading wheelset's lateral displacement y_{wl} for the S1002/UIC60 pair of wheel/rail profiles

Fig. 14. Part two of stability map – peak-to-peak value of leading wheelset's lateral displacement y_{wl} for the S1002/UIC60 pair of wheel/rail profiles

Fig. 15. Part one of stability map – maximum of absolute value of leading wheelset's lateral displacement y_{wl} for the SZDwheel/R65 pair of wheel/rail profiles

Fig. 16. Part two of stability map – peak-to-peak value of leading wheelset's lateral displacement y_{wl} for the SZDwheel/R65 pair of wheel/rail profiles

Table 1. Parameters of the analysed vehicle-track system

Notation	Description	Measurement unit	HSFV1 freight car parameters
m_b	vehicle body mass	kg	30000
m	wheelset mass	kg	2392
$I_{\xi b}$	body moment of inertia; longitudinal axis	kgm^2	51000
$I_{\eta b}$	body moment of inertia; lateral axis	kgm^2	240000
$I_{\zeta b}$	body moment of inertia; vertical axis	kgm^2	222000
I_{ξ}	wheelset moment of inertia; longitudinal axis	kgm^2	1662
I_{η}	wheelset moment of inertia; lateral axis	kgm^2	50
I_{ζ}	wheelset moment of inertia; vertical axis	kgm^2	1662
k_{zz}	vertical stiffness of the 1st level of suspension	kN/m	4100
k_{zy}	lateral stiffness of the 1st level of suspension	kN/m	431
k_{zx}	longitudinal stiffness of the 1st level of suspension	kN/m	2067
c_{zz}	vertical damping of the 1st level of suspension	kNs/m	28
c_{zy}	lateral damping of the 1st level of suspension	kNs/m	56
c_{zx}	longitudinal damping of the 1st level of suspension	kNs/m	0
a	semi-wheel base	m	3,15
h_b	vertical distance between mass centres of wheelset and vehicle body	m	1,175
r_t	wheelset rolling radius	m	0,375
m_t	vertical mass of the rail	kg	200
k_t	vertical stiffness of the rail	kN/m	70000
c_t	vertical damping of the rail	kNs/m	200
m_{ty}	lateral mass of the track	kg	500
k_{ty}	lateral stiffness of the track	kN/m	25000
c_{ty}	lateral damping of the track	kNs/m	500

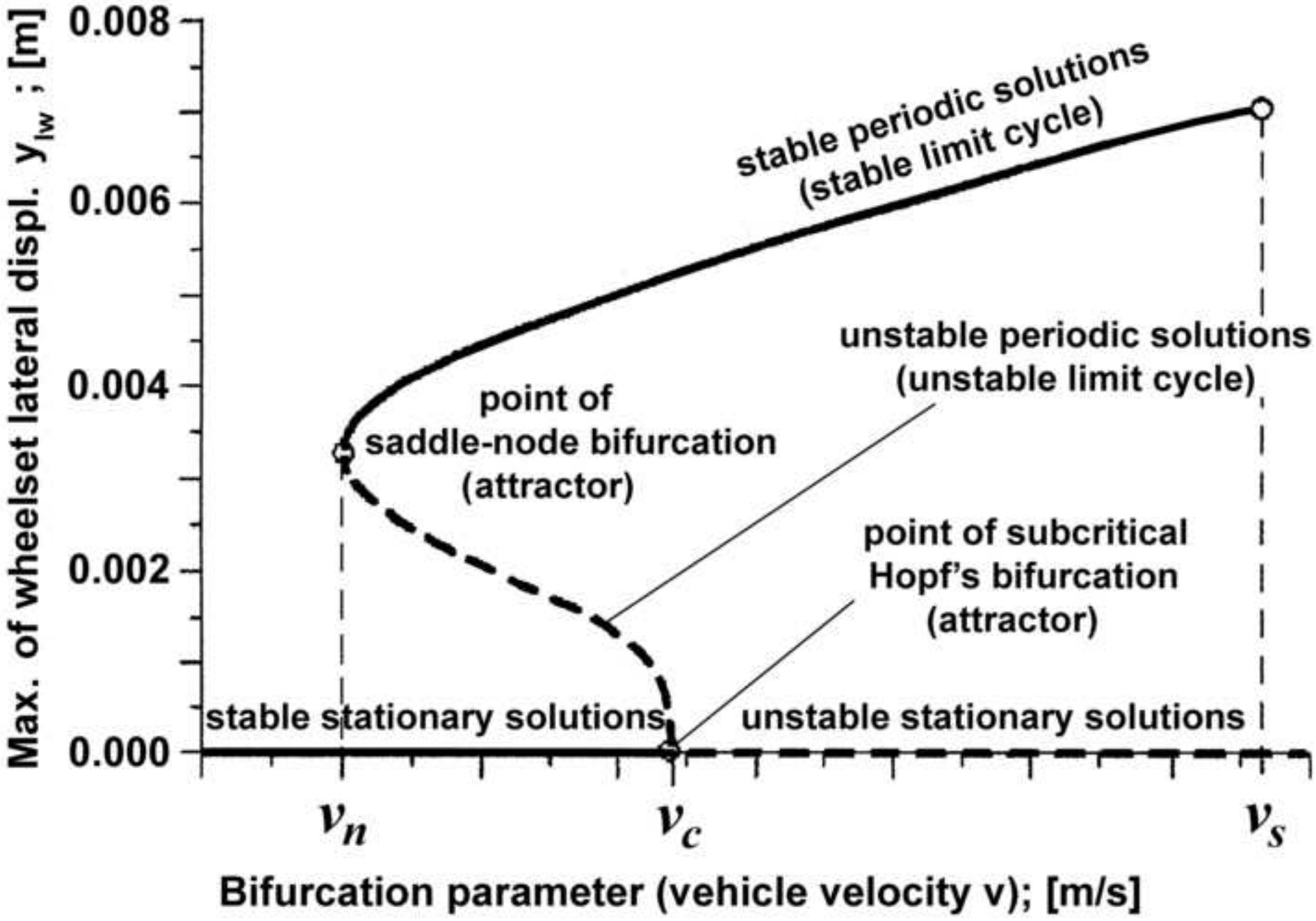
Max. of wheelset lateral displ. y_{lw} ; [m]
0.008
0.006
0.004
0.002
0.000
stable periodic solutions
(stable limit cycle)
unstable periodic solutions
(unstable limit cycle)
point of
saddle-node bifurcation
(attractor)
point of subcritical
Hopf's bifurcation
(attractor)
stable stationary solutions
unstable stationary solutions
v_n
v_c
v_s
Bifurcation parameter (vehicle velocity v); [m/s]

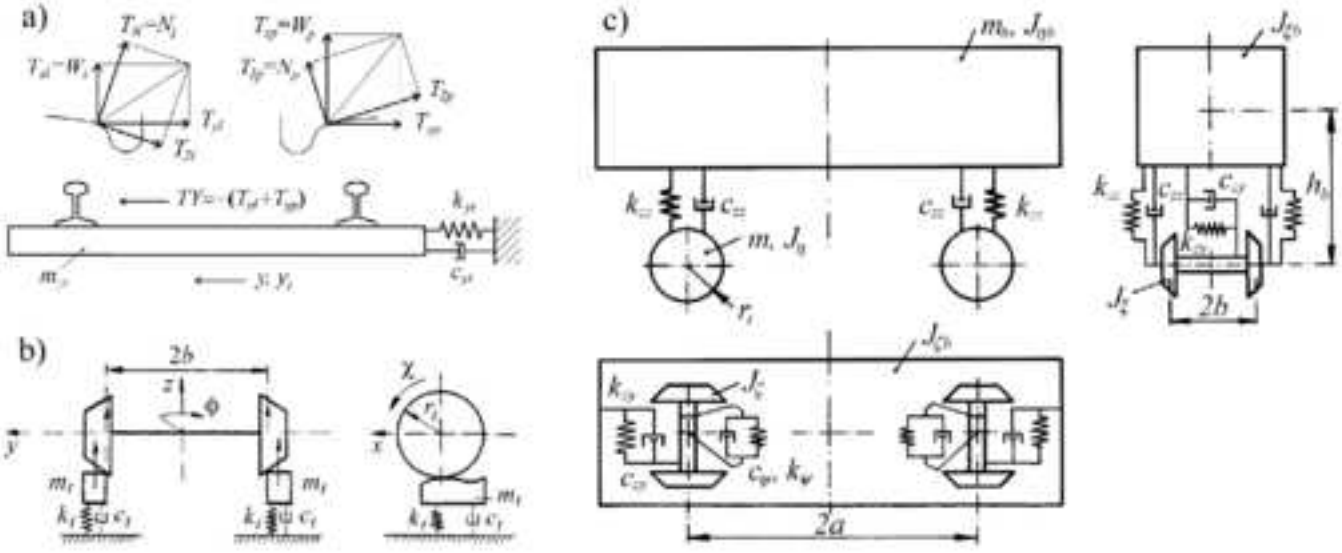

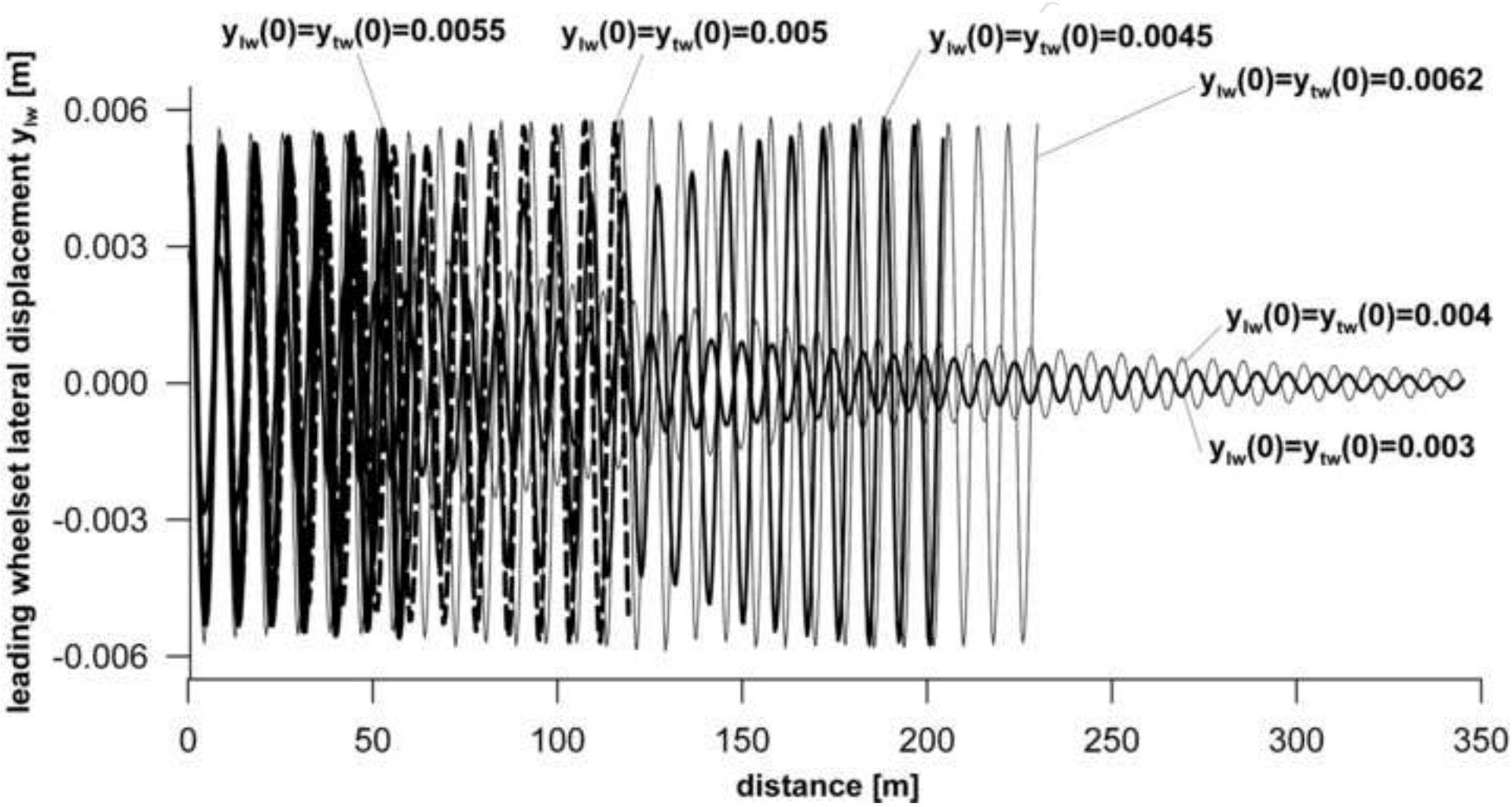
$y_{lw}(0)=y_{tw}(0)=0.0055$
$y_{lw}(0)=y_{tw}(0)=0.005$
$y_{lw}(0)=y_{tw}(0)=0.0045$
$y_{lw}(0)=y_{tw}(0)=0.0062$
$y_{lw}(0)=y_{tw}(0)=0.004$
$y_{lw}(0)=y_{tw}(0)=0.003$
leading wheelset lateral displacement y_{lw} [m]
0.006
0.003
0.000
-0.003
-0.006
0
50
100
150
200
250
300
350
distance [m]

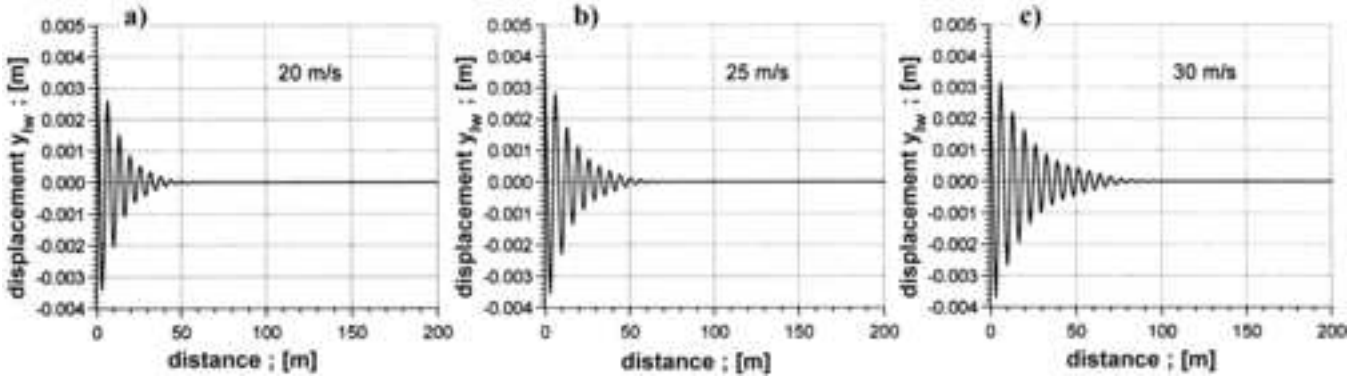

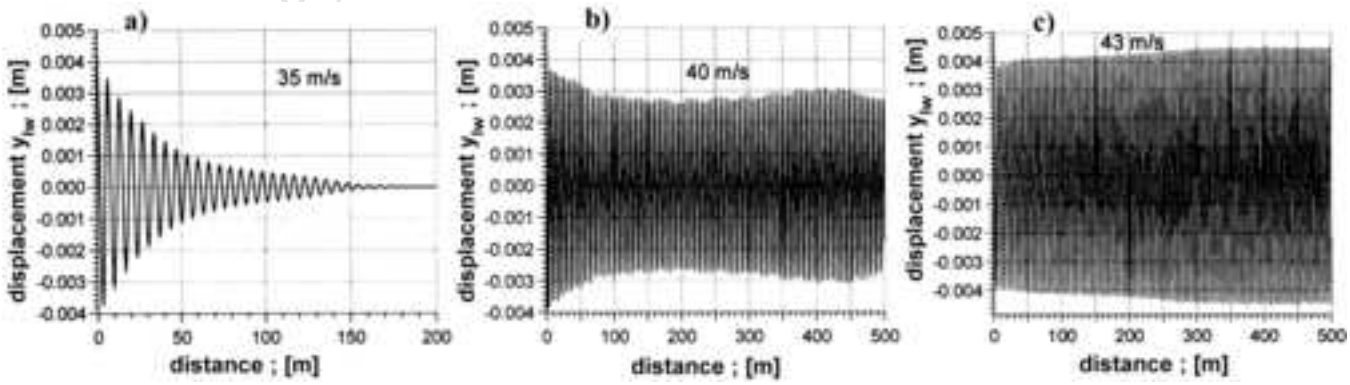

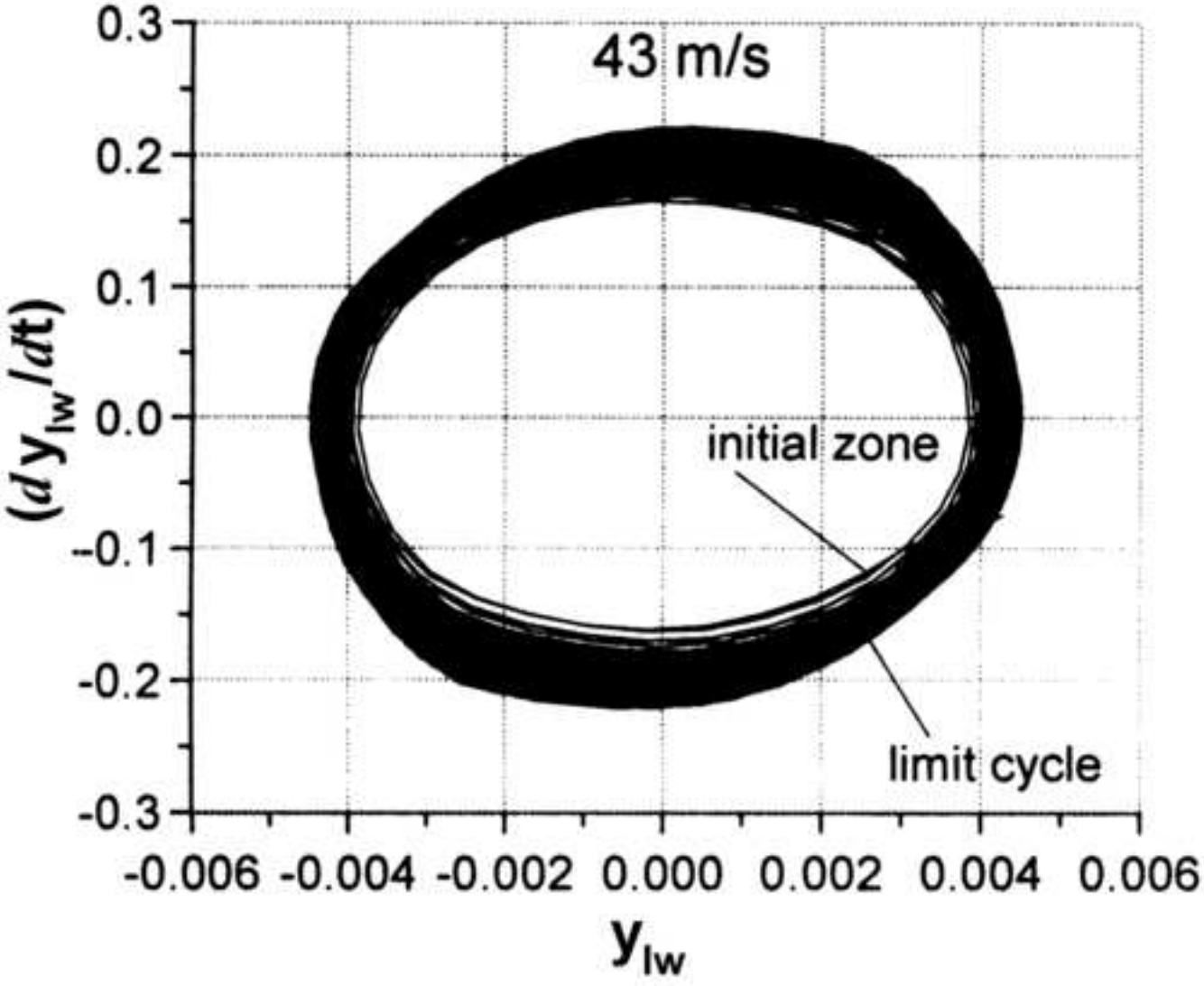
43 m/s
initial zone
limit cycle
0.3
0.2
0.1
0.0
-0.1
-0.2
-0.3
-0.006
-0.004
-0.002
0.000
0.002
0.004
0.006
(dy_{lw}/dt)
y_{lw}

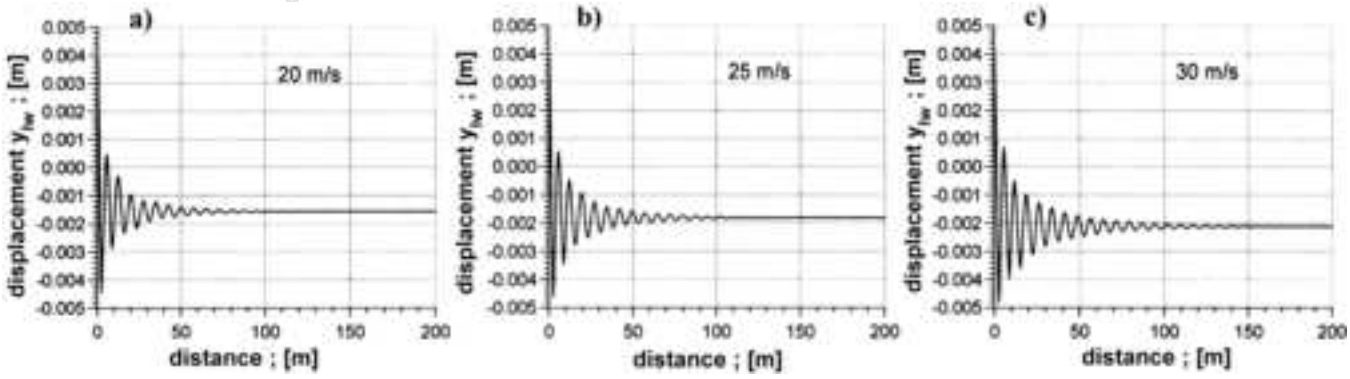

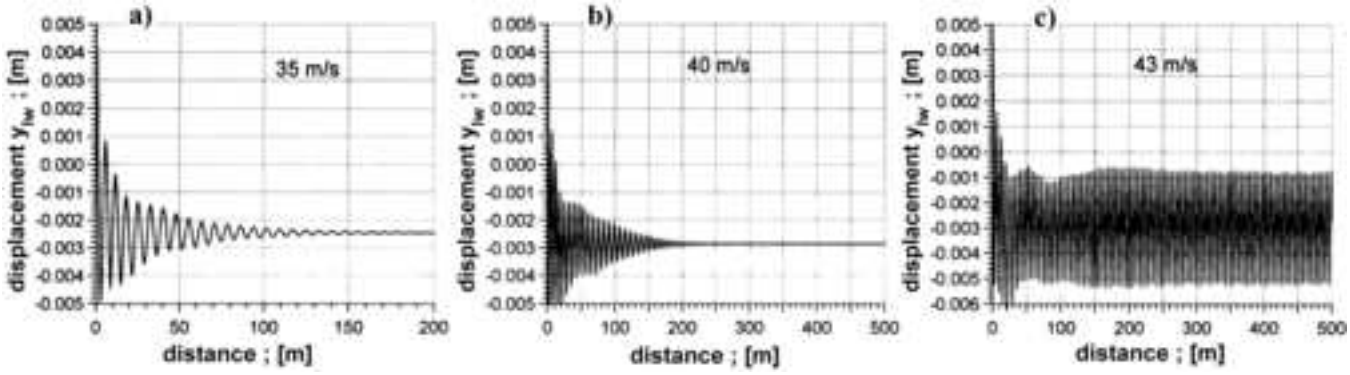

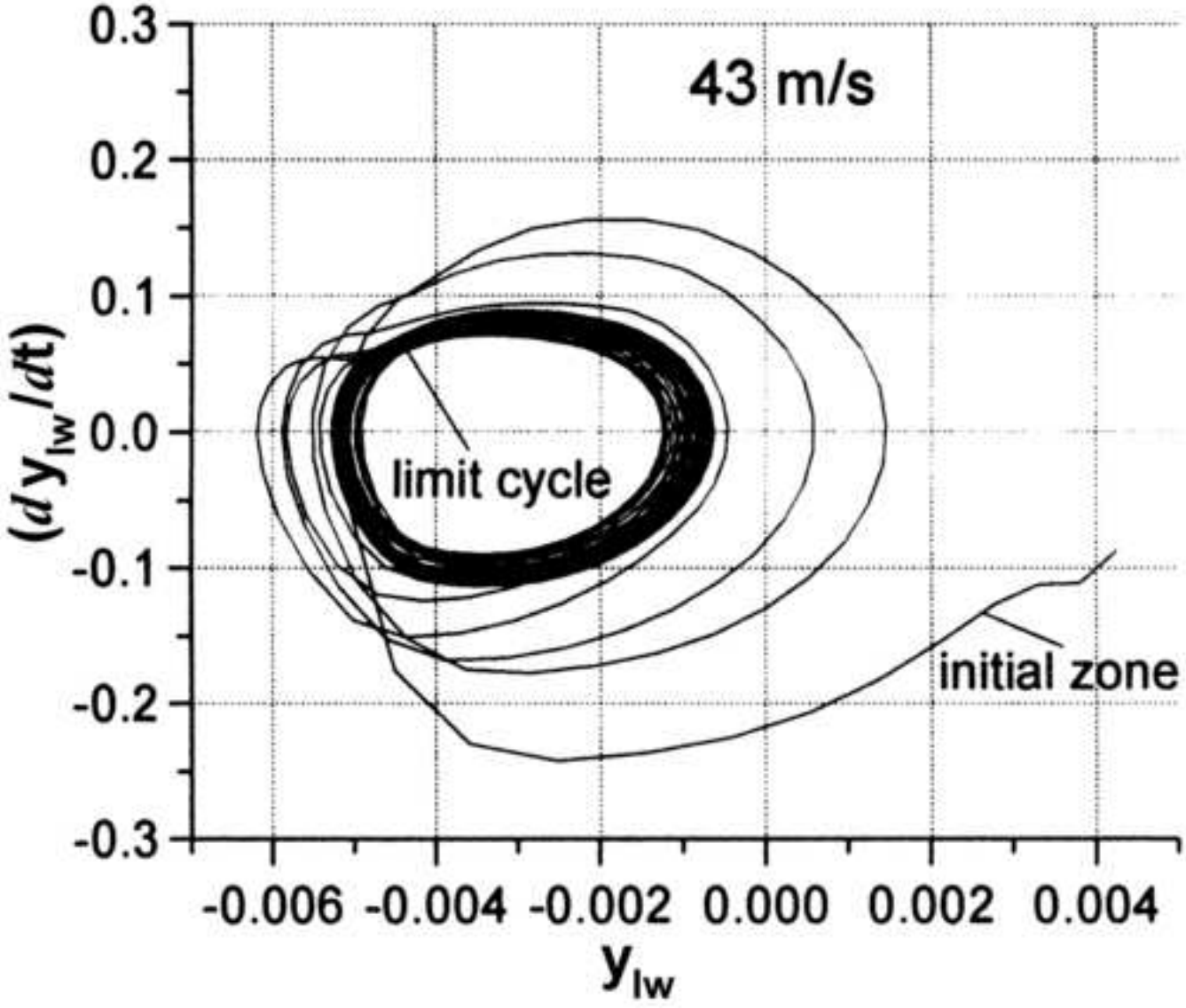
43 m/s
limit cycle
initial zone
0.3
0.2
0.1
0.0
-0.1
-0.2
-0.3
-0.006
-0.004
-0.002
0.000
0.002
0.004
(dy_{lw}/dt)
y_{lw}

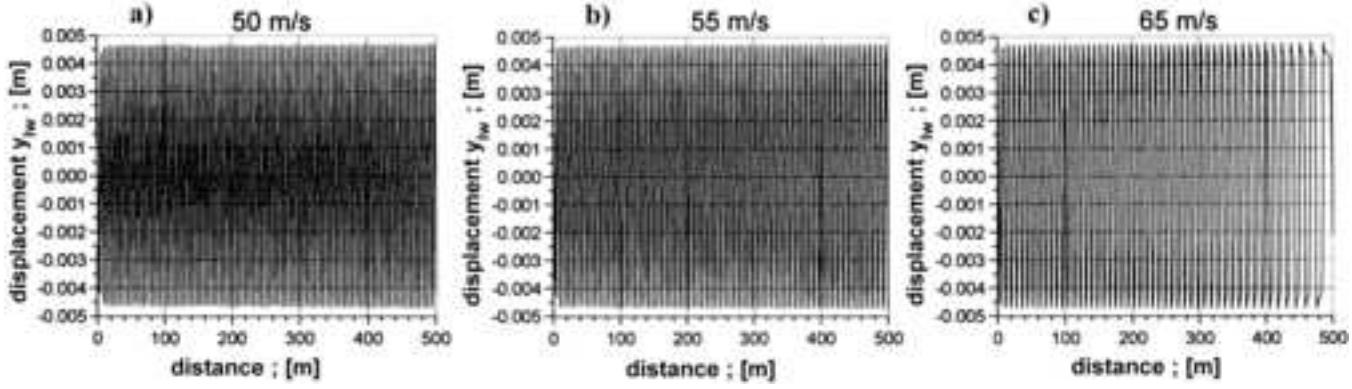

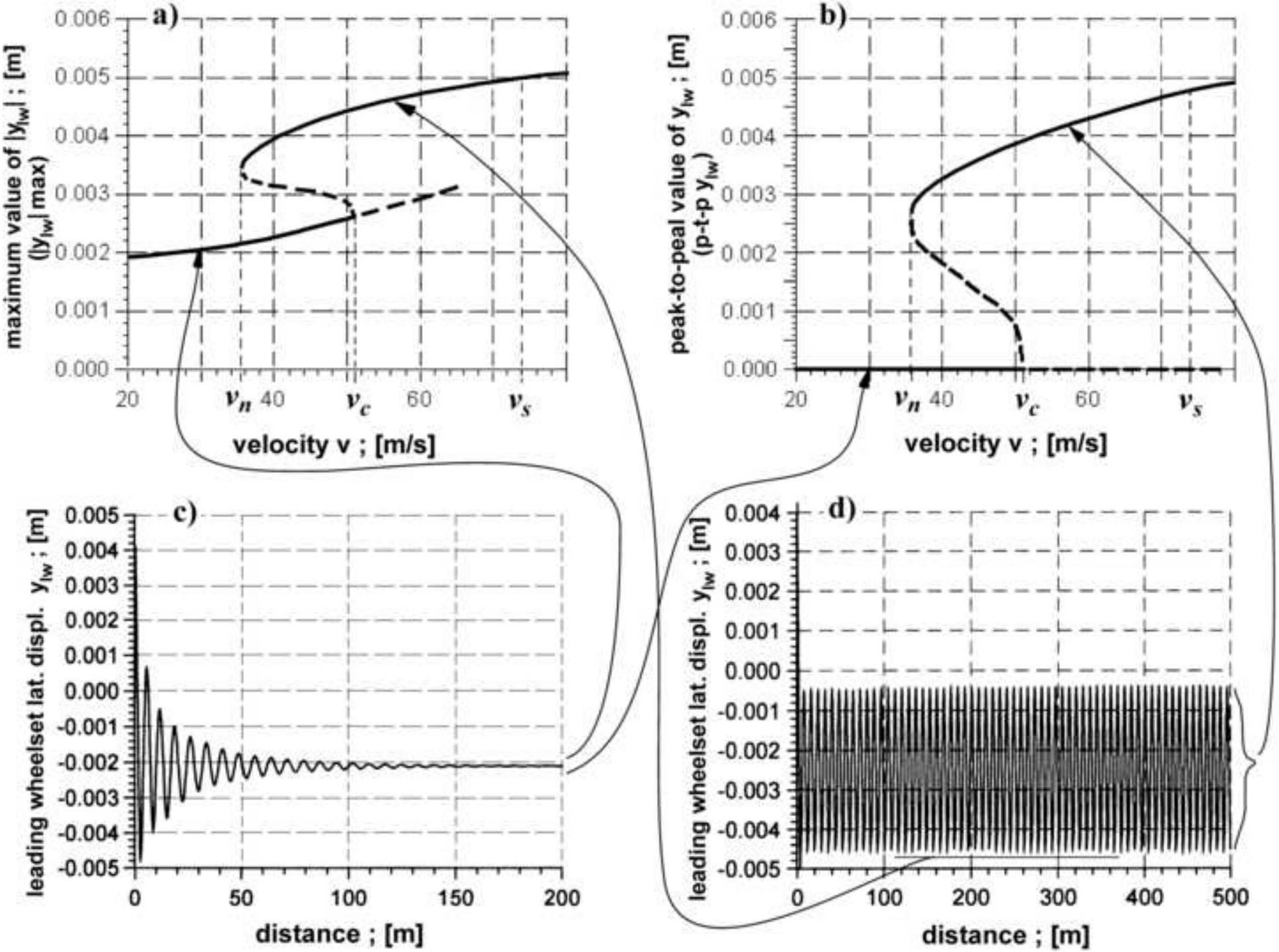
a)
maximum value of |y_lw| ; [m]
(|y_lw| max)
0.006
0.005
0.004
0.003
0.002
0.001
0.000
20
v_n
40
v_c
60
v_s
velocity v ; [m/s]
b)
peak-to-peal value of y_lw ; [m]
(p-t-p y_lw)
0.006
0.005
0.004
0.003
0.002
0.001
0.000
20
v_n
40
v_c
60
v_s
velocity v ; [m/s]
c)
leading wheelset lat. displ. y_lw ; [m]
0.005
0.004
0.003
0.002
0.001
0.000
-0.001
-0.002
-0.003
-0.004
-0.005
0
50
100
150
200
distance ; [m]
d)
leading wheelset lat. displ. y_lw ; [m]
0.004
0.003
0.002
0.001
0.000
-0.001
-0.002
-0.003
-0.004
-0.005
0
100
200
300
400
500
distance ; [m]

Numerical simulation of railway vehicle motion

The procedure for bulding bifurcation plot in type of Fig.1, valid for straight track case

In case of circular curve analysis it is sensible to consider a set of curve radii R rather than single radius R. This might be the following radii R = 300, (450), 600, (750), 900, 1200, 2000, 3000, 4000, 6000 and 10000 m

Track cant H corresponding to particular radius R has to be determined. The question appears how to do it to get the best results in terms of comparison of different simulated cases. It can be assumed in the following ways:

- H - is the same for different velocities and is nominal one for v_n (this option was used in most of our studies),
- H - is nominal one for each v (used in particular simulations),
- other arbitrary choice

Despite solutions typical in straight track also exist for curved track, care must be taken of several types of untypical solutions. These are:

- periodic solutions below velocity v_n (the critical velocity for straight track),
- stationary solutions for whole range of velocities above v_n,
- abrupt jumps from one to another periodic solution,
- jumps from periodic to stationary solution above v_n,
- jumps from stationary to periodic solution above v_n,
- chaotic solutions above v_n

Non-linear critical velocity v_n in circular curve and in straight track appeared to be the same (for the model studied here). Nevertheless, the deviations can appear connected with the untypical solutions listed above or different models

Typical bifurcation plot used for straight track analysis of the stability is not enough in case of the curved track. A pair of the bifurcation diagrams is necessary to give enough information in such conditions of motion. The first diagram corresponds to the diagram used for straight track, however represents maximum of absolute value of wheelset lateral displacement y_{lw}. The second one represents peak-to peak value of y_{lw}

Following the recommendations in the first block joint presentation of the pairs of bifurcation diagrams for **ST** and any value of R is also sensible. This leads to two cumulative bifurcation diagrams that form stability map representing vehicle stability properties in any conditions of motion (in terms of R value)

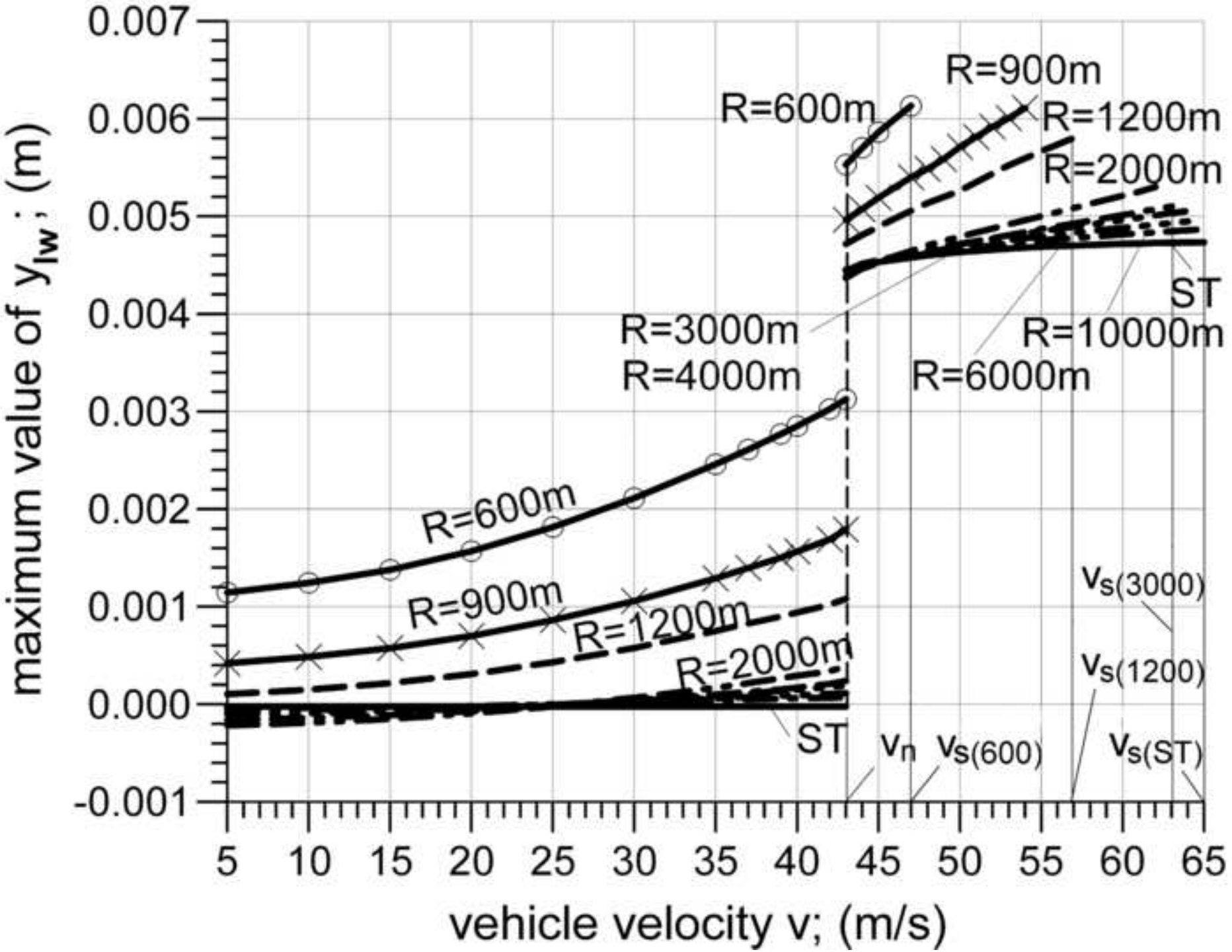
0.007
0.006
0.005
0.004
0.003
0.002
0.001
0.000
-0.001
maximum value of y_{lw}; (m)
5
10
15
20
25
30
35
40
45
50
55
60
65
vehicle velocity v; (m/s)
R=600m
R=900m
R=1200m
R=2000m
ST
R=3000m
R=4000m
R=10000m
R=6000m
R=600m
R=900m
R=1200m
R=2000m
ST
v_n
$v_{s(600)}$
$v_{s(3000)}$
$v_{s(1200)}$
$v_{s(ST)}$

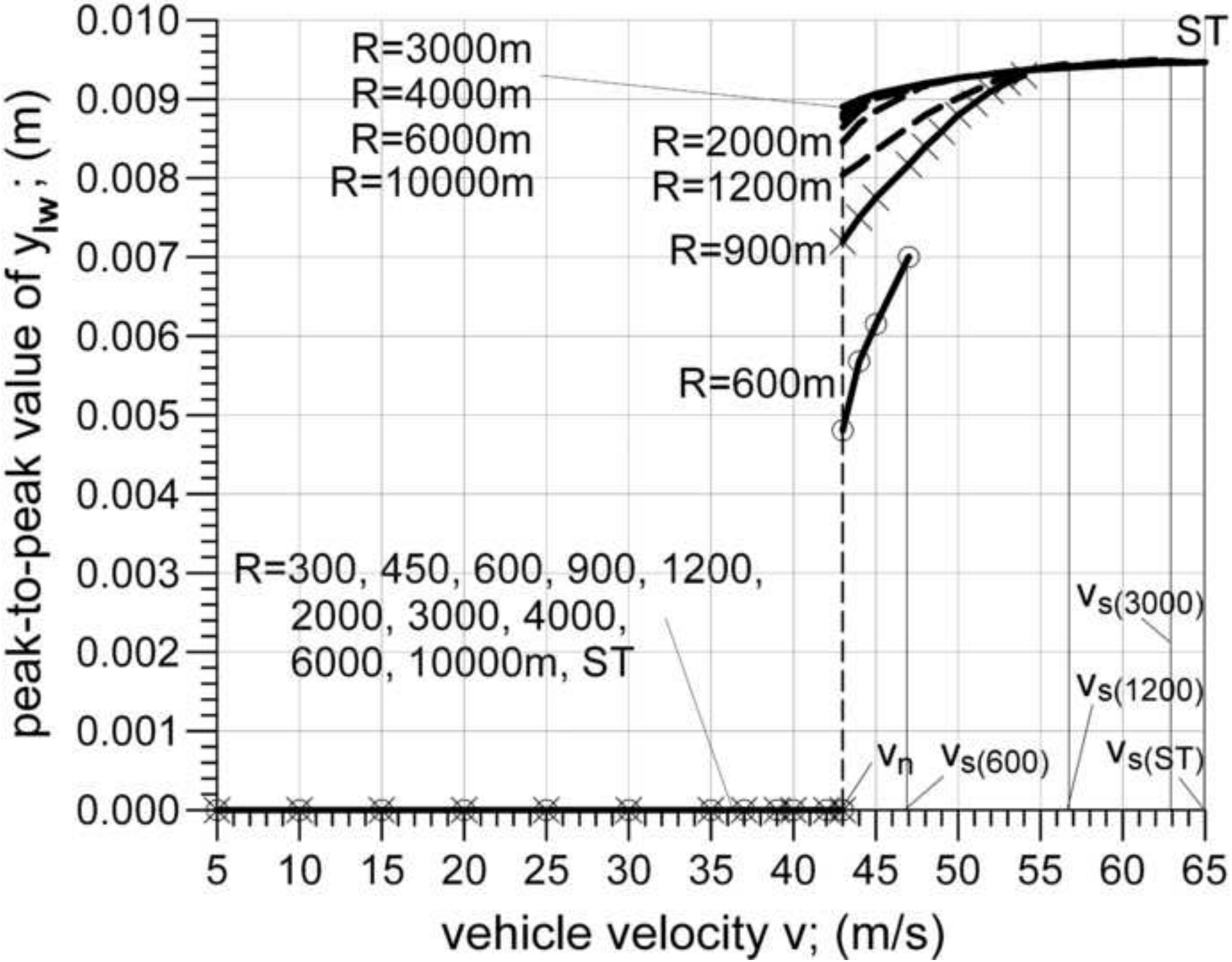
peak-to-peak value of y_{lw}; (m)
0.010
0.009
0.008
0.007
0.006
0.005
0.004
0.003
0.002
0.001
0.000
R=3000m
R=4000m
R=6000m
R=10000m
ST
R=2000m
R=1200m
R=900m
R=600m
R=300, 450, 600, 900, 1200,
2000, 3000, 4000,
6000, 10000m, ST
$V_{s(3000)}$
$V_{s(1200)}$
V_n
$V_{s(600)}$
$V_{s(ST)}$
5
10
15
20
25
30
35
40
45
50
55
60
65
vehicle velocity v; (m/s)

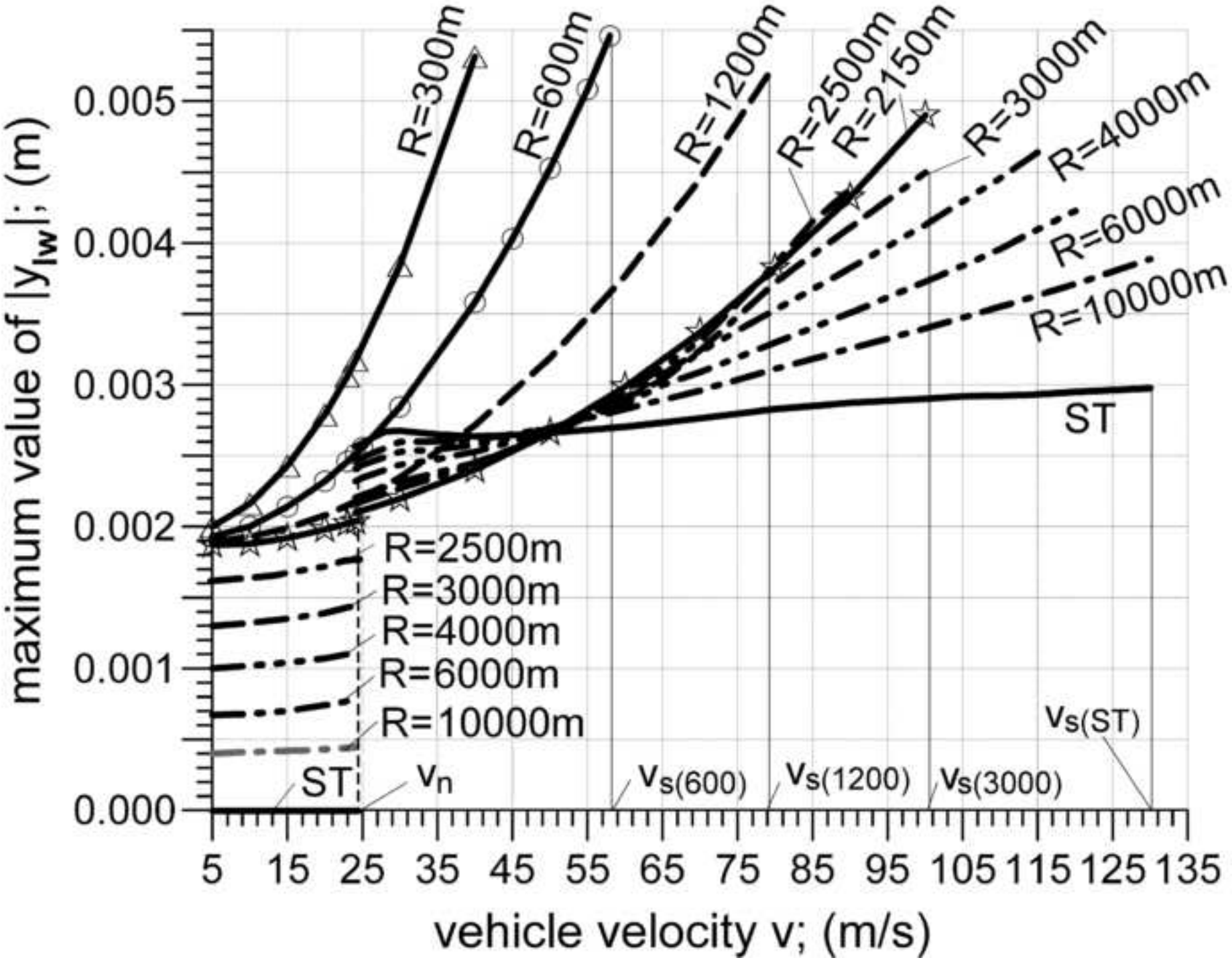
maximum value of |y_lw|; (m)
0.000
0.001
0.002
0.003
0.004
0.005
5
15
25
35
45
55
65
75
85
95
105
115
125
135
vehicle velocity v; (m/s)
R=300m
R=600m
R=1200m
R=2500m
R=2150m
R=3000m
R=4000m
R=6000m
R=10000m
ST
R=2500m
R=3000m
R=4000m
R=6000m
R=10000m
ST
v_n
v_s(600)
v_s(1200)
v_s(3000)
v_s(ST)

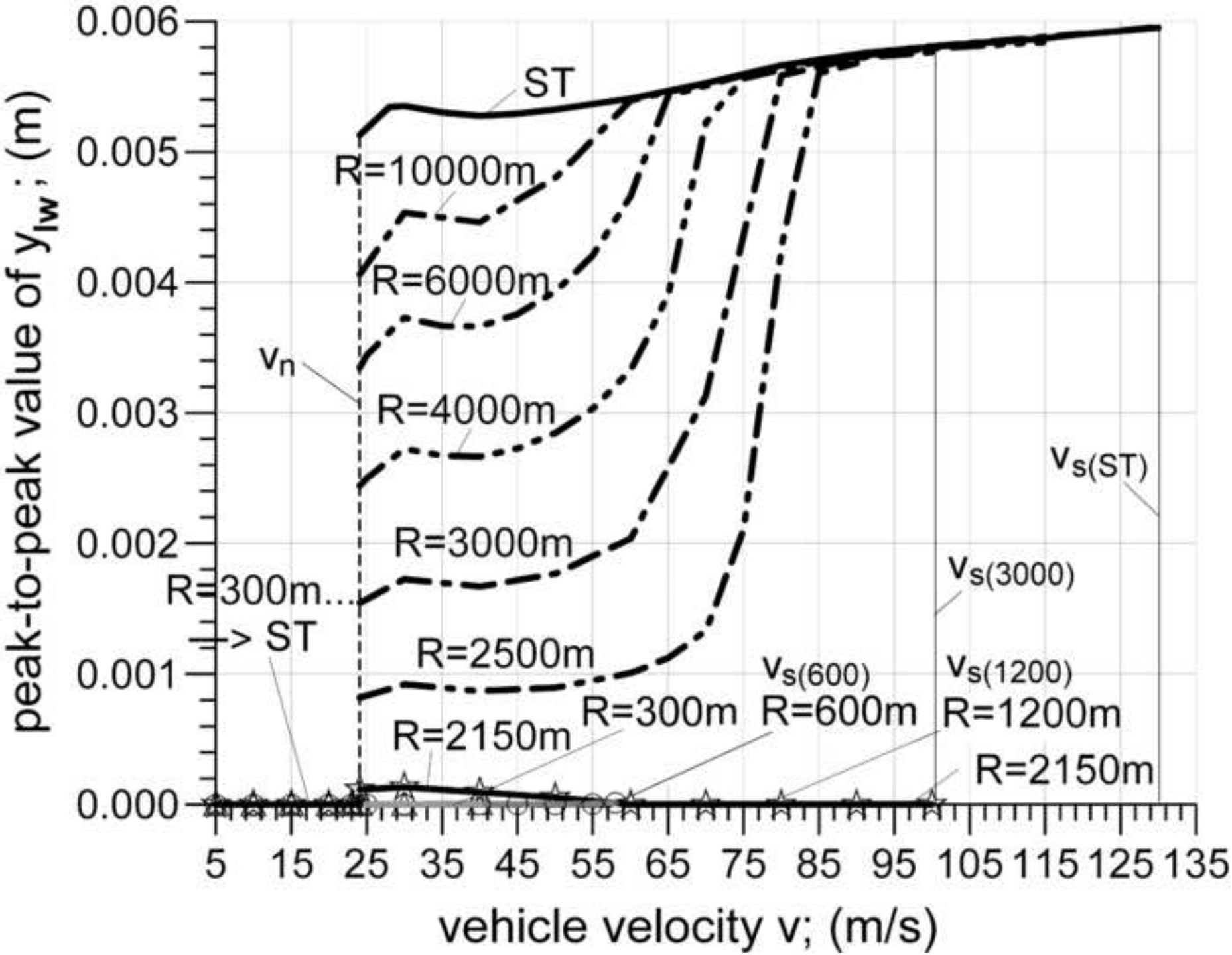
0.006
0.005
0.004
0.003
0.002
0.001
0.000
peak-to-peak value of y_{lw}; (m)
ST
R=10000m
R=6000m
v_n
R=4000m
R=3000m
R=300m...
-> ST
R=2500m
R=2150m
$v_{s(ST)}$
$v_{s(3000)}$
$v_{s(600)}$
$v_{s(1200)}$
R=300m
R=600m
R=1200m
R=2150m
5 15 25 35 45 55 65 75 85 95 105 115 125 135
vehicle velocity v; (m/s)